Identifying Favorable Catalyst Design Features in Methane Steam Reforming using Computational Fluid Dynamics

---

A Major Qualifying Project Report

Submitted to the Faculty of the

WORCESTER POLYTECHNIC INSTITUTE

In partial fulfillment of the requirements for the

Degree of Bachelor of Science

In Chemical Engineering

By

Merlin Nikodemus

_____

Date: April 2013

Approved:

_____

Dr. Anthony G. Dixon, Advisor

ABSTRACT

Steam methane reforming, abbreviated as SMR, is a commonly used process to convert methane into syngas, which is a mixture of hydrogen, carbon monoxide, and carbon dioxide gas. It is the cheapest method of hydrogen production to date and utilized in making hydrogen for fuel cells as well as synthesizing chemical compounds such as ammonia. The SMR process takes place in many long, narrow reactor tubes that are packed with catalysts and externally heated.

This project analyzed the performance of 9 cylindrical catalysts that had 4, 5, or 6 holes and contained a combination of features such as grooves along the length of the cylinder and domed ends. Computational Fluid Dynamics (CFD) was utilized for the analysis since the high reactor operating temperatures inhibit physical experiments. Catalysts were compared by criteria such as pressure drop, heat transfer and reaction rates.

It was concluded that the 5-holed geometries offered a favorable combination of the number of holes and the hole diameter which resulted in low reactor wall temperatures and low pressure drops. It was determined that the 5BHPD geometry, which consisted of 5 wide holes, 5 grooves and domed ends, was the most effective catalyst due to its low pressure drop, high reaction rates, and excellent heat transfer properties.

EXECUTIVE SUMMARY

Steam Methane Reforming (SMR) is a process used to convert methane into syngas, which is a mixture of hydrogen, carbon monoxide, and carbon dioxide. It is widely used in the industry as part of the process in producing ammonia from a natural gas feed and in producing synthetic methanol. SMR is also used to produce hydrogen for use in fuel cells. The reaction kinetics in SMR are highly endothermic, therefore steam reformers are run at high temperatures to produce high reaction rates and a high methane conversion. A steam reformer is made up of many long, narrow fixed-bed reactor tubes with external heating. Most reformers are heated by combustion, usually a natural gas furnace. The reactor tubes are packed with a large number of small catalyst particles, made from a nickel-alumina compound. Catalysts used in the industry are commonly cylindrical of shape and contain various features such as holes and grooves along the length of the catalyst and domed ends.

In order to improve the reforming process the conditions at the inside of the reactor tubes have to be understood and known. However, due to the high temperatures at which SMR takes place, it is difficult to perform physical experimentation. Therefore Computational Fluid Dynamics (CFD) was taken advantage of in order to solve for the transport phenomena such as heat and mass transfer in the system as well as fluid flow. The goal of this project was to identify favorable catalyst characteristics and geometries and find the catalyst shape most suited to be used in SMR under typical conditions. A wide range of 4-holed, 5-holed and 6-holed cylindrical catalysts were studied. The catalyst effectiveness was determined by studying the effect on the pressure drop in the system, the radial heat transfer rate and the reactor wall temperature.

The CFD analysis was performed using the geometry and meshing software GAMBIT and the CFD solver Fluent. A reactor tube model that consisted of a 120° wall segment with a height and diameter of 2 inches was modeled. The model contained 12 particles, but it contained only one complete catalyst particle, located in the center of the tube. This was the test particle that was used to analyze results in this study. Since the solver Fluent did not allow fluid species to be present in solids, it did not support reactions in solids since fluid species would be needed in the catalysts. Therefore the rate equations were written in the C programming language and interpreted into FLUENT before each analysis. User defined scalars were then created that represented the species mass fractions in the system.

A total of nine different geometries were compared in this analysis. Four four-holed geometries, three five-holed shapes, and two six-holed configurations were studied. It is noteworthy to mention that each

catalyst had the same length and diameter to allow for an equal basis for comparison. The two 6-holed geometries used smaller hole diameters in order to make space for the sixth hole. The 5HPD catalyst contains the smallest holes at a radius of only 0.1 inches. All other geometries had hole diameters of 0.1434 inches. The domed ends of the catalysts with such a feature made up 41.6 % of the total catalyst length.

From the results for the wall segment, several catalyst design features were identified. Increasing void fraction of the wall segment led to increased average wall temperatures. The 5BHPD geometry, which contained 5 holes with 5 groves and domed ends, was an exception to this and had the lowest wall temperature out of all catalysts studied. This was explained by its 5 wide holes which redirected flow into the radial direction combined with its larger fluid volume between the catalyst and the reactor wall caused by its domed ends. It was also shown that increasing void fraction led to a lower pressure drop in the system, and the 5BHPD geometry had the second-lowest pressure drop. From the results for the test particles, it was seen that geometric surface area (GSA) of the catalysts with domed ends was lower. However, it was reasoned that these catalysts would pack closer since their volume was less, something not taken into consideration by the wall segment model. Therefore reaction rates per catalyst volume were considered. It was found that the 5BHPD geometry had the highest reaction rates per volume.

Overall, it was concluded that both grooves and domed ends decrease pressure drop but tend to increase reactor wall temperatures. It is also concluded that wider diameter holes are favorable since they decrease pressure drop and encourage radial flow and radial heat transfer. The 5BHPD geometry had the most favorable characteristics and is recommended to be used as the packing pellets in steam reformers. It had a low pressure drop and high reaction rates per volume. It also exhibited excellent radial mixing and radial heat transfer, which resulted in the lowest tube wall temperature and high fluid temperatures. It was recommended that for the domed catalysts, a better wall segment should be developed that more accurately reflects real-life packing patterns.

TABLE OF CONTENTS

ABSTRACT ii
EXECUTIVE SUMMARY iii
TABLE OF FIGURES vii
TABLE OF TABLES viii
CHAPTER 1: INTRODUCTION 1
CHAPTER 2: BACKGROUND 6
2.1 Favorable Reactor and Catalyst Properties 6
2.2 Heat Transfer in the System 7
2.3 CFD Modeling 8
CHAPTER 3: METHODOLOGY 12
3.1 Geometry and Mesh Creation 12
3.2 Setting up the Case in FLUENT 17
3.2.1 Periodic Run 17
3.2.2 Reaction Run 19
CHAPTER 4: RESULTS AND DISCUSSION 22
4.1: Numerical Results 22
4.1.1: Wall Segment Results 22
4.1.2: Test Particle Results 25
4.2: Graphical Results 28
4.2.1: Contours of Temperature on Test Particle 28
4.2.2: Contours of Temperature and Velocity on Iso-Surface 29
4.2.3: Contours of Species Mass Fractions 33
4.2.4: Velocity-Colored Pathlines 34
4.2.5: Radial Temperature Profile 36
4.2.6: Contours of Reaction Rates 39
CHAPTER 5: CONCLUSIONS AND RECOMMENDATIONS 41
REFERENCES 43
APPENDIX A: Convergence Histories 44

A.1: 4H Convergence History 44
A.2: 4HG Convergence History 45
A.3: 4HGD Convergence History 46
A.4: 4HD Convergence History 47
A.5: 5BHPD Convergence History 48
A.6: 5HP Convergence History 49
A.7: 5HPD Convergence History 50
A.8: 6HG Convergence History 51
A.9: 6HGD Convergence History 52
APPENDIX B: BOUNDARY LAYERS APPLIED 53
B.1: 4HD Boundary Layers 53
B.2: 4HGD Boundary Layers 53
B.3: 5HPD Boundary Layers 53
B.4: 5BHPD Boundary Layers 54
B.5: 6HG Boundary Layers 54
B.6: 6HGD Boundary Layers 54
APPENDIX C: PARTICLE LOCATIONS 55
APPENDIX D: SAMPLE GAMBIT JOURNAL FILE 56

TABLE OF FIGURES

Figure 1: Ammonia Process that includes SMR, courtesy of Synetix 2
Figure 2: Previously studied geometries 4
Figure 3: New geometries created 5
Figure 4: The wall segment model 8
Figure 5: Catalyst dimensions 13
Figure 6: Completed model for 5BHPD geometry 14
Figure 7: Meshed 5BHPD geometry 16
Figure 8: Reactor wall temperature versus void fraction for the geometries studied 23
Figure 9: Test particle reaction rates 27
Figure 10: Test particle temperature contours 29
Figure 11: Location of iso-surface, 5BHPD geometry shown 30
Figure 12: Temperature and velocity contours for 4-holed catalysts 31
Figure 13: Temperature and velocity contours for 5 and 6-holed catalysts 32
Figure 14: Contours of methane and hydrogen mass fractions 33
Figure 15: Velocity-colored pathlines for 4-holed catalysts 34
Figure 16: Velocity-colored pathlines for 5 and 6-holed catalysts 35
Figure 17: Location of the line in respect to the iso-surface 36
Figure 18: Temperature profile for 4-holed catalysts 37
Figure 19: Temperature profile for 5 and 6-holed catalysts 38
Figure 20: Reaction rate contours for 5BHPD and 6HG geometries 39

TABLE OF TABLES

Table 1: Main reactions in Steam Methane Reforming 1
Table 2: SMR reaction mechanism 10
Table 3: Catalyst geometry dimensions 12
Table 4: Flow conditions and material properties 17
Table 5: Initialization conditions for periodic run 18
Table 6: Species definitions for reaction run 20
Table 7: Wall segment results 22
Table 8: Test particle results 25

CHAPTER 1: INTRODUCTION

Steam Methane Reforming (SMR) is a process used to produce hydrogen by reacting methane and steam. It is widely used in the industry as part of the process in producing ammonia from a natural gas feed and in producing synthetic methanol. SMR is also useful in producing hydrogen for the growing hydrogen economy, where hydrogen is used in fuel cells to combust with oxygen and create energy with water as the only emission [5]. Hydrogen production by SMR is the cheapest and most common process used to date, and almost all of the 9 megatons of hydrogen produced yearly in the United States are made using SMR. Having been used in the industry for many years, the process is quite efficient at 65-75% efficiency. The SMR process produces syngas, a mixture of hydrogen, carbon monoxide, and carbon dioxide. If pure hydrogen is the desired product, the hydrogen has to be separated from the syngas stream. Syngas production by SMR is dominated by three chemical reactions [6], displayed in Table 1.

Table 1: Main reactions in Steam Methane Reforming

Reaction	Heat of Reaction (kJ/mol)
$CH_4 + H_2O \leftrightarrow CO + 3H_2$	-206.1
$CO + H_2O \leftrightarrow CO_2 + H_2$	41.15
$CH_4 + 2H_2O \leftrightarrow CO_2 + 4H_2$	-165.0

As indicated by the heats of reaction, SMR is a highly endothermic process. In other words, the reaction process absorbs energy when hydrogen is produced. Therefore the reaction rate is proportional with temperature and at higher temperatures the reactions proceeds more rapidly. Chemical process plants that use SMR therefore operate the reactors at high temperatures, often in excess of 700 K to yield high equilibrium conversions and therefore high hydrogen production to maximize profits.

A steam reformer is made up of many long, narrow fixed-bed reactor tubes with external heating. Most reformers are heated by combustion, usually a natural gas furnace. The reactor tubes are packed with a large number of small catalyst particles, made from a nickel-alumina compound. Because of the use of catalysts in SMR, it is important that the feed stream be free of sulfur compounds since they could quickly poison the catalysts. Sulfur is usually removed from the feed stream in the form of hydrogen sulfide gas. Catalysts used in the industry are commonly cylindrical of shape and contain various

features such as holes and grooves along the length of the catalyst and domed ends. A process flow diagram for the production of ammonia is shown in Figure 1, courtesy of Synetix.

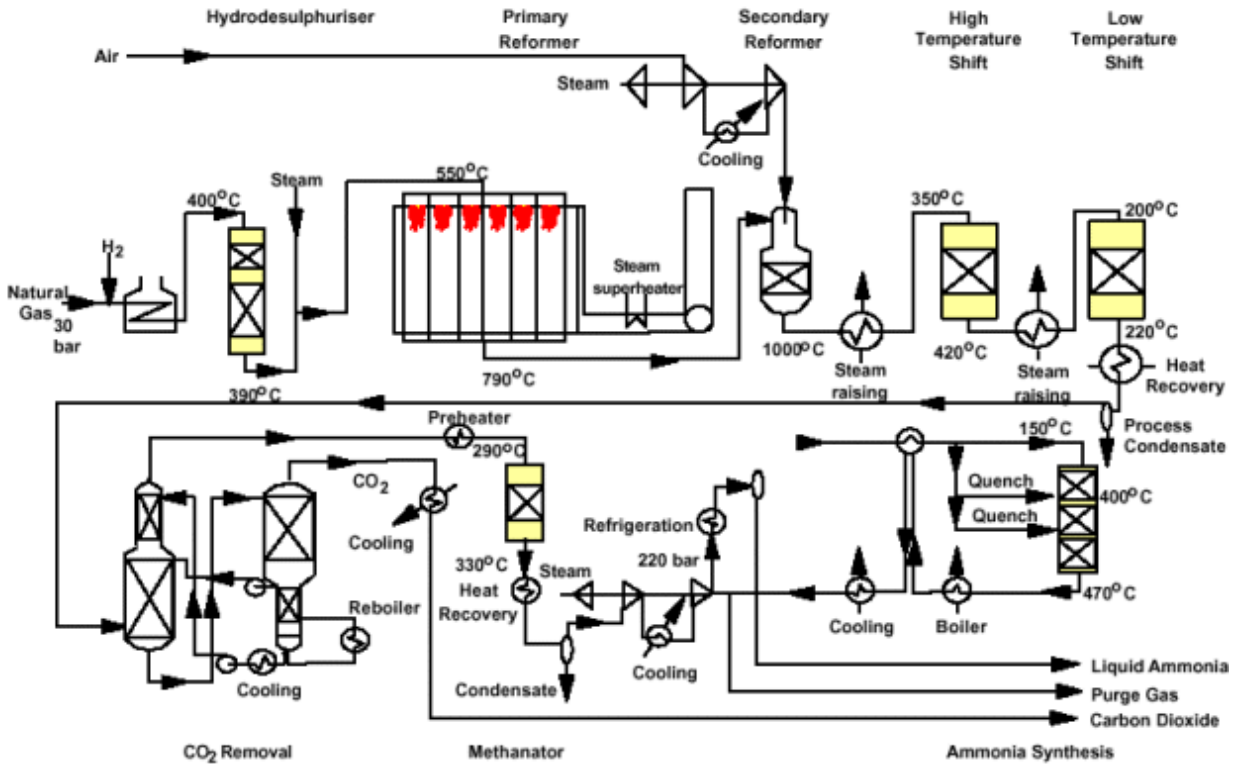

Figure 1: Ammonia Process that includes SMR, courtesy of Synetix

This particular process contains a hydrodesulfuriser in which the natural gas feed stream is mixed with hydrogen gas, heated, and reacted in a catalytic environment to convert sulfur into hydrogen sulfide and remove it from the process. The gas stream is then mixed with steam and flows through the methane-steam reformer, which is a fired unit made up of several tubes as previously mentioned. Eventually the hydrogen produced in the reformer unit reacts with nitrogen to produce ammonia.

It should be noted that syngas contains a significant amount of carbon dioxide; therefore the CO_2 usually has to be captured and separated from the gas stream in order to reduce emissions and follow environmental regulations. There is a significant cost associated with this [8].

In order to improve the reforming process and further increase its efficiency, the conditions of the inside of the reactor tubes have to be understood and known. However, due to the high temperatures at which SMR takes place, it is difficult to perform physical experimentation. Therefore Computational

Fluid Dynamics (CFD) is taken advantage of in order to solve for the transport phenomena such as heat and mass transfer in the system as well as fluid flow.

The goal of this project is to identify favorable catalyst characteristics and geometries and find the catalyst shape most suited to be used in SMR under typical conditions. A wide range of 4-holed, 5-holed and 6-holed cylindrical catalysts are studied. A CFD analysis is performed using the geometry and meshing software GAMBIT and the CFD solver Fluent is used to solve for the heat and mass transfer, fluid flow, and reactions in the system. The catalyst effectiveness was determined by the studying the effect on the following characteristics:

- $Heat\ transfer$- higher heat transfer results in higher reaction rates and longer tube life
- $Pressure\ drop$- lower pressure drop means higher product flow
- $Methane\ production$- higher methane reaction rate means more product and more profit

An important geometric characteristic which correlates with reaction rate is the ratio of surface area to volume. Since the reactions in SMR are heterogeneous, they take place on the surface of the catalyst and not in the fluid volume as in homogeneous reactions. Therefore a higher surface area means there are more catalyst sites available for reactions to occur. As a result, a higher surface area to volume ratio means a higher reaction rate and therefore more hydrogen is produced in a given amount of time.

Another defining geometric characteristic of a catalyst shape is its associated void fraction in the packed bed. This is a fraction between 0 and 1 that is calculated by dividing the volume of void space in the bed by its total volume. A higher void fraction means that at equal mass flow through the system, the available volume for the fluid to flow through is higher, which results in lower fluid velocity and therefore lower pressure drop.

To optimize these two defining characteristics, there has been a shift in the industry from spherical catalysts which are easy to manufacture and offer high surface area to cylindrical pellets with a variation of holes [1]. Cylindrical shapes are favorable because it is easy to add holes to these catalysts without compromising their structural integrity. This makes for high surface areas and high void fractions. The holes through the length of the catalyst also increase the available pathways for fluid to travel through and funnel fluid flow in multiple directions. This mixes the fluid inside the reactor and makes for efficient heat transfer.

Therefore the geometries that are studied in this CFD analysis are all cylindrical shaped with various holes and grooves along the length of the pellet. A total of nine catalyst geometries are analyzed, three of which were previously studied [3][4]. The three geometries which were created previously are shown in Figure 2.

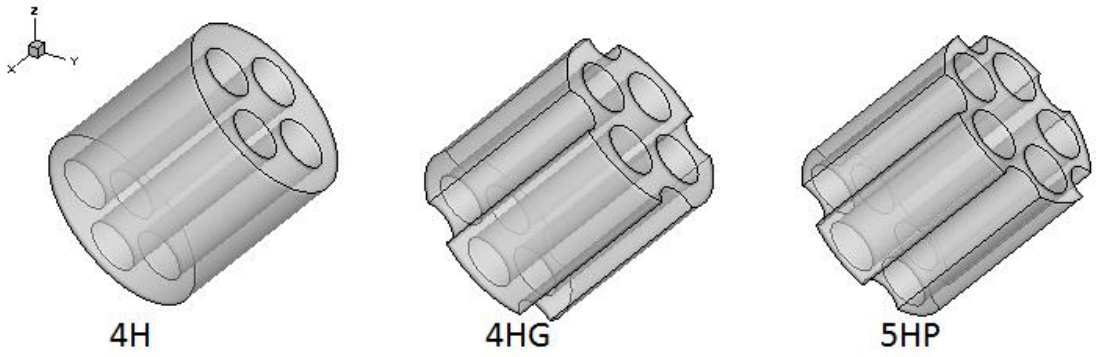

Figure 2: Previously studied geometries

The 4H geometry is simply a cylinder with four holes through the length of the catalyst, arranged in a square. The 4HG geometry is that of the 4H with the addition of four grooves along the length of the cylinder arranged in a square that is rotated 45 degrees from the positions of the holes. In the previous study [3], it was concluded that the 4HG geometry is the most favorable out of a variety of 1, 3, 4 and 6 holed geometries. The 6-holed geometry was concluded to be the second choice. However, it should be noted that the 6-holed geometry studied did not include grooves and therefore had a lower void fraction, which was the main argument against it. The 5HP geometry contains 5 holes arranged in a pentagonal shape with 5 grooves also arranged pentagonal and offset from the holes. In the previous study [4], this geometry was found to be the most favorable out of a variety of 5-holed geometries. The geometries created in this study are presented in Figure 3.

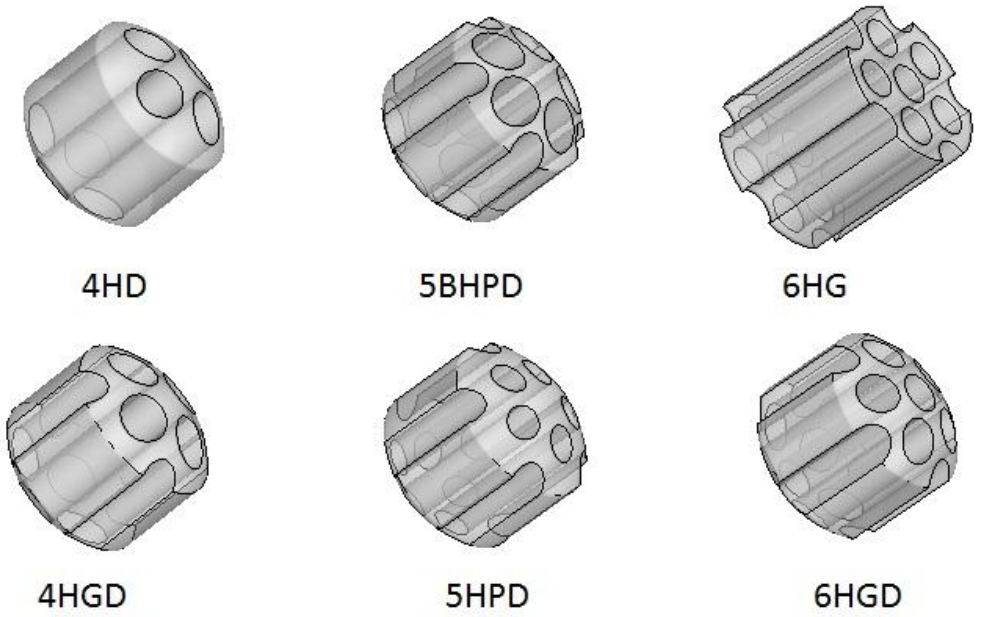

Figure 3: New geometries created

All catalysts studied had an equal diameter to length ratio and were one inch in maximum length and one inch in diameter. Figure 3 can give the impression that the domed geometries are shorter than the other catalysts, this is however not the case and simply an optical illusion. Each catalyst geometry is briefly described below:

- $4HD$- this geometry features four holes aligned in a square shape plus domed ends.
- $4HGD$- this catalyst is similar to the 4HD geometry with the addition of four grooves.
- $5BHPD*$- this shape features five holes and five grooves arranged in a pentagonal pattern plus domed ends
- $5HPD*$- this is similar to the 5BHPD shape with the modification of smaller diameter holes. This geometry has the same hole diameter as the 6HG and 6HGD catalysts.
- $6HG$- this catalyst contains five holes and grooves arranged in a pentagonal pattern with the addition of a sixth hole running through the center of the catalyst.
- $6HGD$- this geometry is the 5HPD geometry with the addition of a hole through the center of the catalyst.

*Note: The orientation of these models is the mirror image of the other models. This was caused by the way the 5HPD geometry was adopted from the previously created 5HP geometry. This has no implications on CFD results, however.

CHAPTER 2: BACKGROUND

2.1 Favorable Reactor and Catalyst Properties

This CFD analysis focuses solely on the geometry of catalysts used in the packing of the reactor tubes used in SMR. Therefore it is important to describe a few of the features of an effective catalyst. These are listed below, with brief descriptions.

Low Pressure Drop- As described previously, a lower pressure drop through the reactor tubes allows for higher flow rates of gas through the system. As a result, more of the feed stream can be processed and converted into syngas. Pressure drop varies inversely with void fraction, meaning that a higher void fraction is favorable since it makes for a lower pressure drop. A higher void fraction means there is more void volume in the system through which the fluid can travel. As a result, the same volume of fluid can travel through the system at a lower velocity, decreasing pressure drop.

High Surface Area: Since the SMR reaction is a heterogeneous chemical reaction; it does not take place in the volume of the fluid but on reaction sites in the catalyst. The reaction is strongly diffusion-limited; therefore the reactions take place overwhelmingly on the outside surface of the catalyst. Consequently, a higher surface area makes for more reaction sites on which the reaction can occur. This increases methane conversion and produces more hydrogen.

Strength of catalyst: The catalyst particles have to be able to withstand the forces from the weight of the particles above each catalyst as well as the violent turbulent forces exerted on them by the fluid flowing through the reactor tubes. In addition to these forces they also need to hold up to the thermal stresses put onto them by the high temperature conditions. If these catalysts begin to disintegrate they increase pressure drop in the reactor significantly by decreasing void fraction in the system and clogging up the reactor tube. The strengths of the various geometries are not studied in this analysis, however.

Radial Mixing: Reactor tubes are externally heated, so it is important that energy is transferred from the tube walls to the fluid and the catalysts since the reaction is highly endothermic and consumes thermal energy. An indicator of efficient radial mixing is a uniform temperature profile of the fluid in the radial direction.

As a side note, it should be said that most of these characteristics interfere with each other. For example, a high surface area is achieved by producing catalysts that contain holes and grooves. This, on the other hand, decreases the structural strength of the catalyst. The goal for a catalyst is to perform reasonably well in each of the categories listed above.

2.2 Heat Transfer in the System

The heat transfer from the furnace throughout the whole system is achieved by shell-side heating, conduction, and convection. The process is explained in more detail below.

Shell-side heat transfer: The reactor tubes are externally heated, usually by means of a furnace. It is important to maintain a relatively constant high tube wall temperature in order to maintain high reaction rates in the endothermic SMR process. A constant tube wall temperature also decreases the thermal stresses on the system. Reactor tube overheating can have dramatic negative effects on performance [12].

Tube wall heat transfer: Heat is transferred through the reactor wall by means of thermal conduction. The coefficient of thermal conductivity, which is a property of the material of the reactor tube, dictates this heat transfer rate.

Fluid heat transfer: Thermal energy is transferred from the inside tube surface to the center by means of radial convection, as mentioned before. It is important to have good heat transfer in order to reduce tube wall temperature and achieve a relatively uniform temperature profile. Energy is then transferred from the fluid to the catalysts, where the endothermic reaction consumes this energy.

2.3 CFD Modeling

Computational Fluid Dynamics (CFD) involves computer modeling software that can be applied to a wide range of engineering disciplines. It relies on the finite volume method (FVM) to solve the underlying differential equations that describe the fluid flow and heat transfer in the system. Rapid improvements in computing capacity and power made for equal rapid improvements in CFD and allows for more complex models to be accurately solved.

In this CFD analysis, the model that was desired is that of a packed bed reactor containing catalyst particles. However, a typical reactor tube is several feet in length and contains a large number of particles. Even with today's computing power, this system would be much too large to effectively model in a CFD study. Therefore only a short section in the center of one of these tubes was studied. A challenge was to produce a model that includes realistic packing of catalysts. Another requirement was that the faces on the top and the bottom of this section are equal. This was needed to be able to define periodic conditions in the CFD solver in order to establish a realistic velocity profile in a flow-only run.

A previous study has created such a model that fulfills the necessary requirements [7]. The model consisted of a 120° wall segment with a height and diameter of 2 inches. The top and bottom faces are exactly equal and the catalyst particles are oriented realistically. The complete model for the 5BHPD geometry is represented in Figure 4.

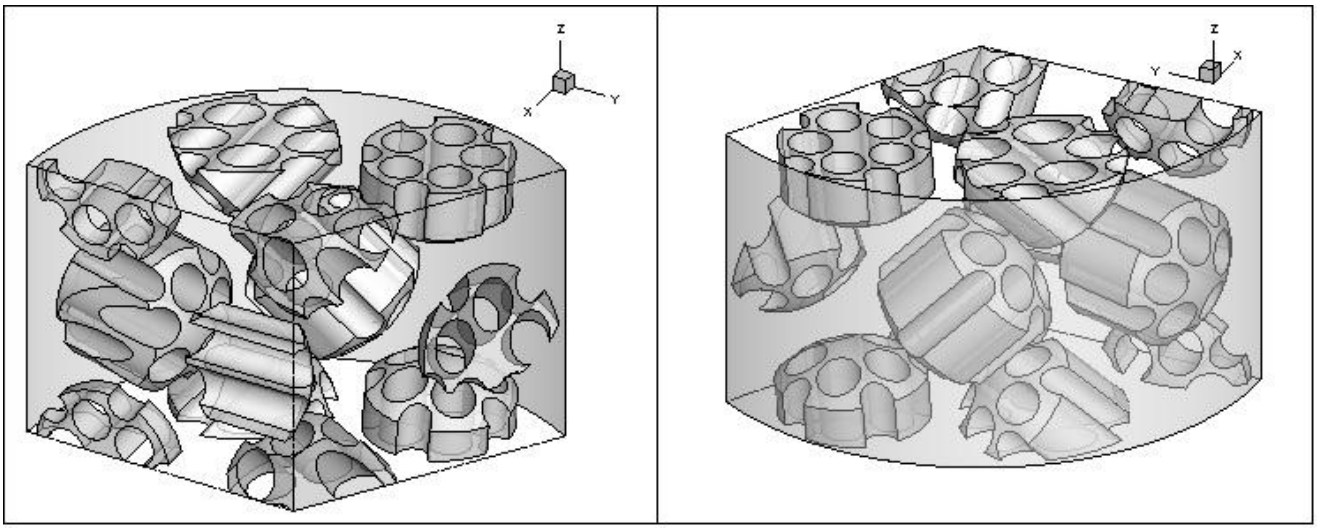

Figure 4: The wall segment model

It is important to note that the model only contains one catalyst particle that is complete, located in the center of the tube. This is the test particle that was used to analyze results in this study.

Turbulent Flow Modeling

To solve for the turbulent fluid flow through the tube segment, the proper turbulent flow model needs to be selected. Previous models that were used, such as the k-ε model, were not accurate in modeling turbulent flow throughout the system. Instead of solving the differential equations for fluid flow until the solid surface is reached, this model made use of wall functions to estimate near-wall fluid behavior based on empirical equations. The relatively recent developed SST k-ω model is much more accurate in solving for fluid behavior [10]. The k-ω model is accurate in solving for fluid flow near solid walls. This is especially important in this study because fluid behavior close to catalyst walls can have a large impact on reaction kinetics, and inaccuracies in this part of the model can lead to skewed results. However, the k-ω model is not as accurate in modeling bulk fluid flow. Therefore the SST k-ω was developed which virtually separates fluid flow into two zones, one containing the bulk fluid flow and one containing near-wall flow. It then applies the k-ω and k-ε models to the flow regions in which they are the most accurate, resulting in a more accurate and realistic flow solution for the model.

Diffusion Modeling

The CFD solver used in this study, FLUENT, does not allow fluid species to be present in solid zones. To accurately model the system, user defined functions were developed in previous studies [7]. These utilize user defined scalars to represent the mass fractions of each species within the system, which are then determined by the subroutines present in the user defined functions. During each iteration that the solver performs, these user defined functions are executed. The functions are written in the C programming language and then simply loaded into the CFD solver for interpretation. Studies using CFD code have used this approach before and validated their results [1].

Reaction Kinetics

A reaction mechanism for SMR has been developed by Hou and Hughes [9]. It consists of 9 elementary reaction steps with three rate limiting steps. The mechanism is represented in

Table 2.

Table 2: SMR reaction mechanism

Step Number	Reaction
s1	$H_2O + s \leftrightarrow H_2 + Os$
s2	$CH_4 + 3s \leftrightarrow CH_2s + 2Hs$
s3	$CH_2s + Os \leftrightarrow CHOs + Hs$
s4 (Rate Limiting)	$CHOs + s \leftrightarrow COs + Hs$
s5 (Rate Limiting)	$COs + Os \leftrightarrow CO_2s + s$
s6 (Rate Limiting)	$CHOs + Os \leftrightarrow CO_2s + Hs$
s7	$COs \leftrightarrow CO + s$
s8	$CO_2s \leftrightarrow CO_2 + s$
s9	$2H_2 \leftrightarrow H_2 + 2s$

Hou and Hughes developed final rate equations for the limiting reaction steps. The Langmuir-Hinshelwood-Hougen-Watson (LHHW) approach was used to develop the equations below [9].

$$r_1 = \frac{k_1 \left(\frac{P_{CH_4} * P_{H_2O}^{0.5}}{P_{H_2}^{1.25}} \right) \left(1 - \left(\frac{P_{CO} P_{H_2}^3}{K_{P1} P_{CH_4} P_{H_2O}} \right) \right)}{DEN^2}$$

$$r_2 = \frac{k_2 \left(\frac{P_{CO} * P_{H_2O}^{0.5}}{P_{H_2}^{0.5}} \right) \left(1 - \left(\frac{P_{CO_2} P_{H_2}}{K_{P2} P_{CO} P_{H_2O}} \right) \right)}{DEN^2}$$

$$r_3 = \frac{k_3 \left(\frac{P_{CH_4} * P_{H_2O}}{P_{H_2}^{1.75}} \right) \left(1 - \left(\frac{P_{CO_2} P_{H_2}^4}{K_{P3} P_{CH_4} P_{H_2O}^2} \right) \right)}{DEN^2}$$

Where

$$DEN = 1 + K_{CO}P_{CO} + K_H P_H^{0.5} + K_{H_2O}\left(\frac{P_{H_2O}}{P_{H_2}}\right)$$

It can be seen that each rate equation contains an equilibrium constant k and the partial pressures of various species. These factors together determine the overall rate of the reaction. The denominator present in all three rate equations, DEN, accounts for the adsorption of all species on the catalyst surface.

Using the Arrhenius and van't Hoff equations, Hou and Hughes were also able to determine equations for the rate and equilibrium constants. These are shown below.

$$k_i = A_i e^{-\left(\frac{E_i}{RT}\right)}$$

$$K_i = A(K_i)e^{-\left(\frac{\Delta H_{i,a}}{RT}\right)}$$

As mentioned before, the CFD solver Fluent does not allow fluid species to be present in solids. As a result, it also does not support reactions in solids since fluid species would be needed in the catalysts. Therefore the rate equations were written in the C programming language and included in the file containing the user defined functions, making use of the user defined scalars to represent species mass fraction in the solid catalysts.

CHAPTER 3: METHODOLOGY

3.1 Geometry and Mesh Creation

The models developed in this CFD study are based on a 2 inch portion of a reactor tube. Only a 120° wedge was studied, and the radius of the wedge is 2 inches as well. The wedge contains two symmetry planes and equal top and bottom faces. The bottom and top faces were meshed identically so that periodic conditions could be specified in the solver. The model contains 12 particles, out of which only one catalyst, particle 2, is complete. All other catalysts extend out of the reactor wedge and are therefore cut off from the model. Therefore particle 2 is used as a test particle and kinetics results are based off particle 2. A total of 6 different catalyst geometries were created, with either 4,5 or 6 holes and various combinations of grooves and domed ends. The ratio of the tube to particle diameter (the N value) is equal to 4. This agrees with the low range of N values for packed bed reactors as noted previously by Nijemisland, Dixon and Stitt [6]. The geometry and mesh were created using GAMBIT 2.4.6.

Creation of first particle

The geometry creation was initialized by designing one single catalyst. Six different catalyst geometries, as previously shown in Figure 3, were created. Information about geometry features such as hole and groove diameters are presented below in Table 3. All dimensions are given in inches.

Table 3: Catalyst geometry dimensions

Geometry	Length	Diameter	Hole Radius	Groove Radius	Dome Radius
4HD	1	1	0.1434	NA	0.70496
4HGD	1	1	0.1434	0.12	0.70496
5BHPD	1	1	0.1434	0.11	0.70496
5HPD	1	1	0.1000	0.11	0.70496
6HG	1	1	0.1200	0.12	NA
6HGD	1	1	0.1200	0.12	0.70496

It is noteworthy to mention that each catalyst had the same length and diameter to allow for an equal basis for comparison. Each measured 1 x 1 inches. The two 6-holed geometries used smaller hole diameters in order to make space for the sixth hole. The 5HPD catalyst contains the smallest holes at a radius of only 0.1 inches. The domed ends of the catalysts with such a feature made up 41.6 % of the total catalyst length. The dimensions of domed catalysts and geometries without domes are presented in Figure 5.

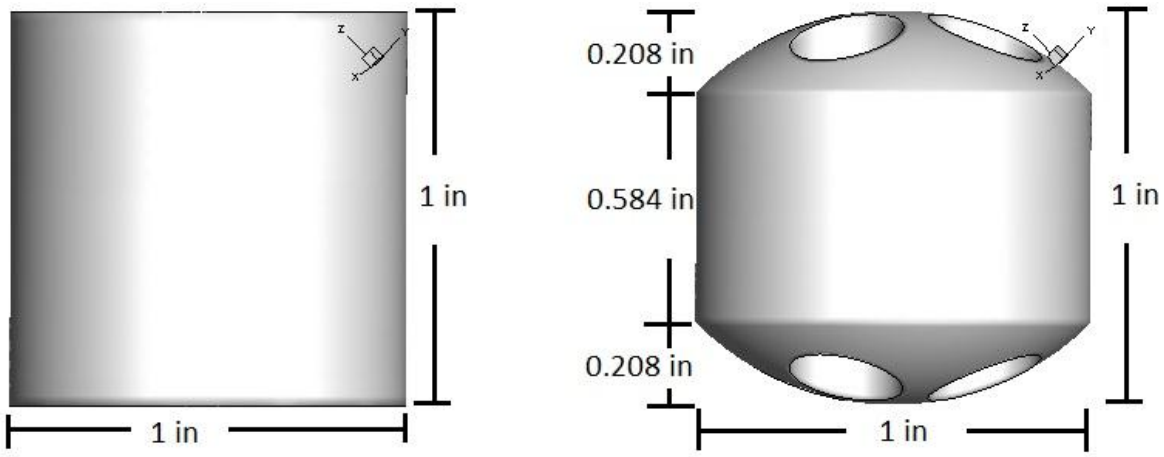

Figure 5: Catalyst dimensions

The strategy used to model each catalyst was the top-down approach. This meant rendering basic shapes and volumes and creating particles out of these shapes, compared to the bottom-up approach where vertices and lines are used to create faces and then stitch faces into volumes. First a cylinder volume was created. For the domed particles, two spheres were created and then moved to the appropriate positions at the top and bottom of the cylinder. These spheres were then each split with the top and bottom faces of the cylinder, creating domed ends. These ends were then united with the cylinder volume to form one volume. Additionally, holes were created by creating cylinders with the appropriate diameters and then moving them in the correct positions within the catalyst shape. These cylinders were then subtracted from the main volume to create a holed catalyst particle. Grooves were created using this same strategy.

Base Geometry

In order to fill the wedge with the remaining 12 catalyst particles, the first particle was copied twelve times and each copy was translated and rotated to its correct position within the reactor tube segment.

The original particle was then deleted. The translation and rotation information used in this process can be found in Appendix C. A completed model for the 5BHPD geometry is shown below in Figure 6.

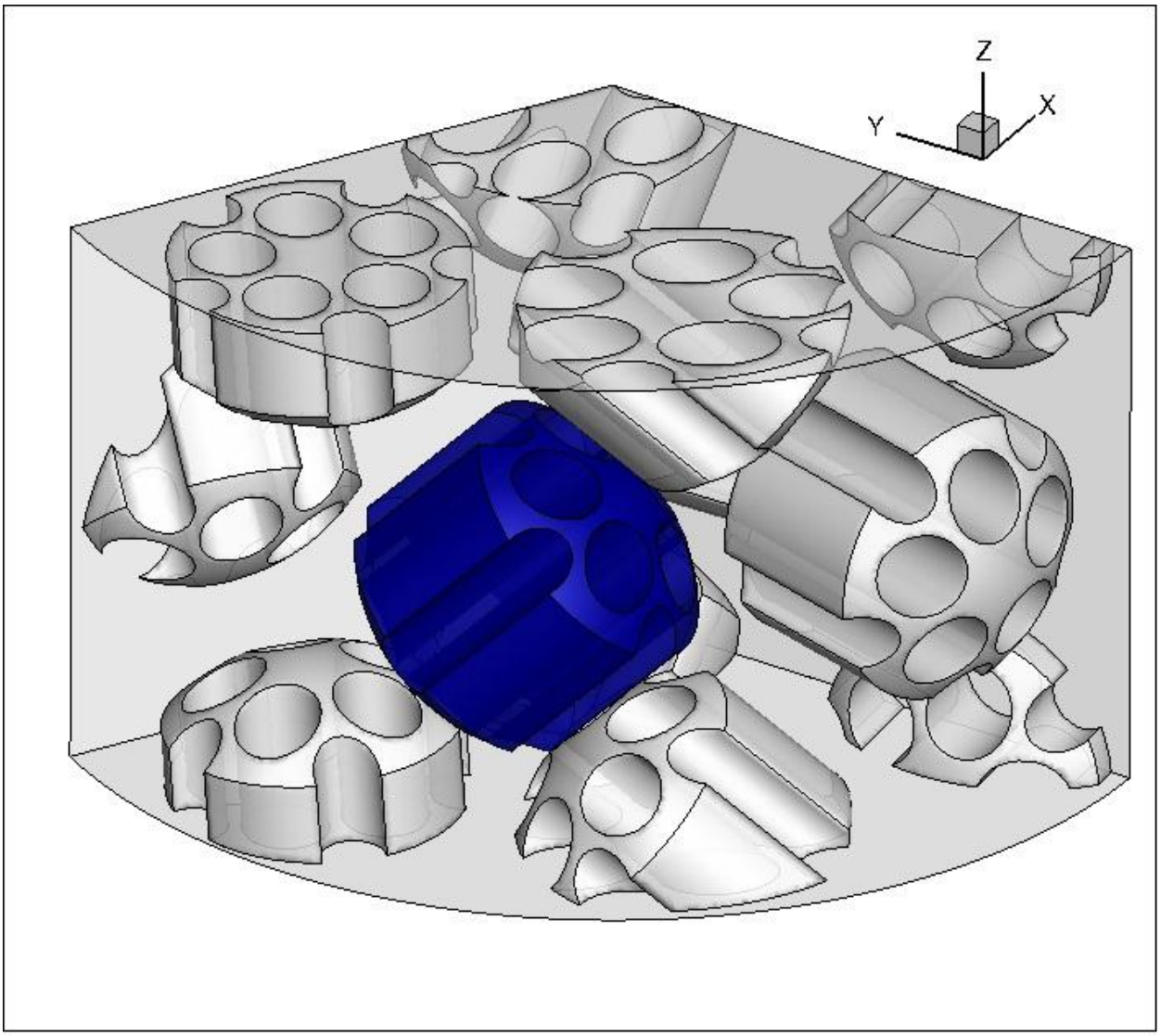

Figure 6: Completed model for 5BHPD geometry

Each particle was then split with the main cylinder volume. This prevented the need to connect faces from the cylinder volume and the catalyst volumes. The next step was to label each face for future reference. Each face was named so that it would be easy to identify later on, therefore the name included the particle name and an identifier such as “hole” or “top-end”.

Face Linking

In order to define periodic conditions in Fluent, the top and bottom faces of the reactor tube segment have to be meshed exactly the same. Therefore all top and bottom faces have to be linked for meshing so that GAMBIT only creates one mesh and then copies it to the corresponding face. Each pair of faces on the top and bottom planes was linked using reverse orientation.

Boundary Layers

Boundary layers were added to a few of the catalyst particles. These varied from geometry to geometry, with the only constant being that particle 2, the test particle, always contained boundary layers. Boundary layers determine the mesh size near solid and fluid boundaries. This is important because a refined mesh is necessary in near-wall areas since viscous models and the no slip boundary conditions are very sensitive in these areas. The boundary layer input in GAMBIT is defined by the first layer size, the growth factor, and the number of rows. The total depth of the boundary layer is automatically calculated. Various boundary layers were used in the six geometries, and they are listed in Appendix B. Boundary layer size and presence is specific to each geometry. Boundary layers were limited by the prominent "edge intersects face" error message in GAMBIT. This occurred when a boundary layer intersected a face in the geometry. Therefore the boundary layer size had to be reduced or in some cases completely removed. In the 5BHPD geometry, boundary layers were only applied to the test particle because GAMBIT's meshing scheme was especially sensitive to boundary layers and failed when they were applied to any other particles.

Meshing the Model

The entire model was meshed in GAMBIT using triangle elements for faces and tetrahedral elements for volumes. The element size was usually 0.03 inches, but in some instances volumes had to be meshed finer to prevent boundary layers from intersecting faces and to prevent skewed elements in the model. This was especially prevalent in regions with small volumes and odd shapes produced by splitting the catalyst volumes with the wall segment. All solid and fluid volumes were meshed and a mesh file was then written using the export feature in GAMBIT. The meshed 5BHPD geometry is shown below in Figure 7.

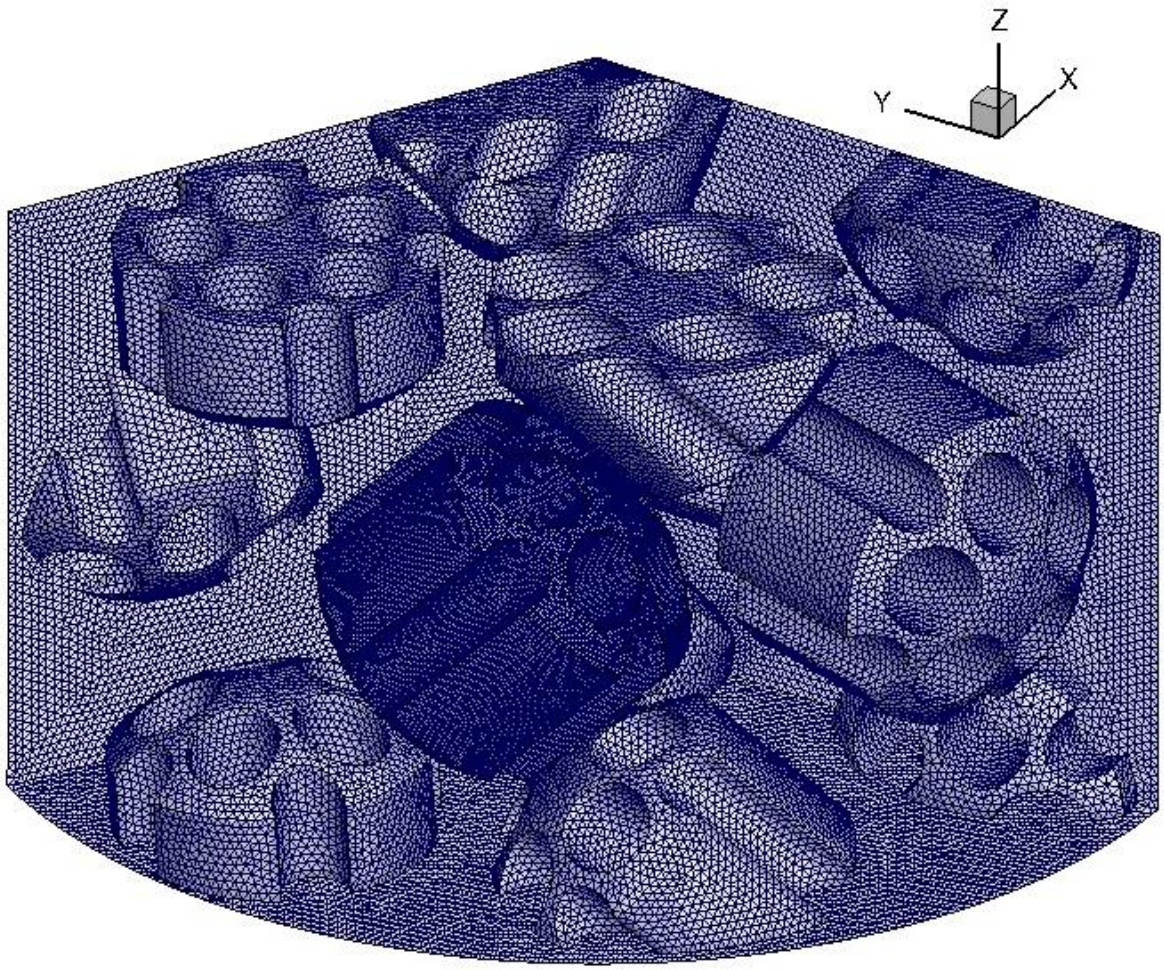

Figure 7: Meshed 5BHPD geometry

It is important to note that the test particle was meshed much denser than the rest of the system. This is why it looks darker than the other catalyst particles in the figure. As previously mentioned, particle 2 is the test particle and is used to compare the various geometries against each other. This is why it was meshed finer so that CFD results would be more accurate in this area while saving computing space in other, less dense areas where results do not need to be as refined. A sample GAMBIT input file is presented in Appendix D.

3.2 Setting up the Case in FLUENT

Each geometry was solved in FLUENT 6.3.26. The following outlines the procedure used to set up the case in FLUENT for each model.

3.2.1 Periodic Run

In order to establish a realistic velocity inlet profile, each model was first set up as a periodic case. FLUENT solved only for flow equations and a profile for the top face was written to be used in the reaction run.

Solver Setup

The mesh file created in GAMBIT earlier was read into FLUENT. The mesh was created in inches, but FLUENT's default units are SI, so the grid first had to be scaled. Then the various models were identified, such as the Green-Gauss node-based solver and the SST k-omega model with transitional flows.

Reactor Conditions

Generic reactor operating conditions were chosen, as did previous studies [3]. These are summarized below in Table 4.

Table 4: Flow conditions and material properties

Inlet Feed Temperature (K)	**Reactor Wall Heat Flux (W/m^2)**	**Operating Pressure (Pa)**	**Inlet Velocity (m/s)**
824.15	113,300	2,159,000	3.2
Fluid Properties			
Heat Capacity (J/kg K)	**Thermal Conductivity (W/m K)**	**Viscosity, M (Pa s)**	
2395.38	0.0876	3.0E-05	
Solid Properties			
Heat Capacity (J/kg K)	**Thermal Conductivity (W/m K)**	**Density (kg/m^3)**	
1000	1	1947	

The fluid properties are based on the mix of methane, hydrogen, carbon monoxide, carbon dioxide, and water vapor present in the reactor. The temperature of the reactor is high at 824.15 K to result in a high reaction rate.

Boundary Conditions

Every CFD solver needs a set of boundary conditions in order to solve for the underlying differential equations in the system. Each interface between the fluid and solid faces were set to the "Wall" boundary condition. The top and bottom faces were modified to periodic conditions, with a specified mass flow of 0.02677 kg/s. The cylinder wall has a heat flux of 113,300 W/m^2, but in the flow-only run the energy equations are not solved, therefore this does not have to be specified.

Solution Initialization and Iteration

In order for FLUENT to start solving the case, it first needs initial values to start its iteration process. Values for the viscous model as well as a temperature and velocity profile are needed. The initialization values used are shown in Table 5 below.

Table 5: Initialization conditions for periodic run

Temperature (K)	Inlet Velocity (m/s)	Turbulent Kinetic energy (m^2/s^2)	Specific Dissipation Rate (s^{-1})
824.15	3.2	0.256	43000

After the case is initialized, a specified number of iterations can be performed. However, first solution monitors were implemented. Residuals were plotted for each iteration, and once the residuals stopped changing it could usually be concluded that the flow solution was converged. A statistical solution monitor was also defined, the periodic pressure gradient. This monitor plotted the pressure gradient between the two periodic faces after each iteration. The flow-only runs usually converged after 2000-3000 iterations.

Flux Reports

In order to make sure the solution was actually converged, the mass balance was checked. FLUENT has the option to report fluxes, so the mass flux was calculated for the periodic faces. If this value was very

close to 0, the solution was confirmed converged. A profile was then written that included the x velocity, y velocity, z velocity, turbulent kinetic energy and specific dissipation rate for use in the reaction run as the inlet conditions.

3.2.2 Reaction Run

The reaction run was set up next for each geometry. To do this, the periodic conditions of the flow-only case were undone. This was achieved by using the text command “grid modify-zones slit-periodic”. The bottom face was defined as a velocity inlet and the top face was defined as a pressure-outlet with zero gauge pressure. The transport of species models is enabled in fluent and the five species are defined to be in the mixture.

Initial Setup

The user defined functions specified in the file written in the C programming language were interpreted into fluent in order to calculate the species mass fractions and reaction rates in the system. This file also contains several “Execute on Demand” functions that can be manually executed from the FLUENT user interface as a post-processing feature. They include a function to calculate the total heat sink of the test particle in Watts and a function to calculate the three reaction rates over the test particle’s surface. Four user defined scalars are then defined in all zones, and two user defined memory spaces.

Reactor Conditions

The reactor conditions are the same as before, with a few additions. The initial mass fractions of four of the five reactants have to be specified as well as the mass diffusivities of the species and the solid material. Only four user defined scalars are used to define the mass fractions of methane, hydrogen, carbon monoxide, and carbon dioxide. The mass fraction of the last species, water vapor, can be found by subtracting the four known mass fractions from 1, therefore it is unnecessary to define. The information for the user defined scalars, mass fractions and diffusivities is presented in Table 6.

Table 6: Species definitions for reaction run

User Defined Scalar	Species	Mass Diffusivity (m^2/s)	Mass Fraction
0	Methane	1.23E-05	0.1966
1	Hydrogen	2.25E-05	0.0005
2	Carbon Monoxide	7.20E-06	0.0007
3	Carbon Dioxide	4.90E-06	0.1753
NA	Water Vapor	2.09E-05	From balance

The mass diffusivities presented in the table are used by FLUENT to determine the overall diffusivity of the fluid in the mixture. Also, the user defined functions utilize the diffusivities of each species to calculate a diffusivity value within both the fluid and solid zones of the model.

Boundary Conditions

Several boundary conditions were defined for the reaction run. The bottom face was defined to be a velocity inlet, and its velocity profile was defined by specifying components, and then selecting the appropriate variable from the defined profile. The x velocity was set as the x velocity from the profile, and the specific dissipation rate was set to that of the profile, etc. The top face was set as a pressure outlet at zero gauge pressure. The turbulent kinetic energy and specific dissipation rate for the backflow were also specified to be that of the profile from the periodic case.

For the species transport across solid and fluid interfaces, the appropriate boundary conditions were set as well. As mentioned before, FLUENT does not allow fluid species inside solid zones, which is why user defined functions are used. The user defined scalars account for species within the fluid and the solid. In order to maintain continuity of these user defined scalars and make sure they are equal on each side of the interface, user defined subroutines are needed which then define these values. This assures that the species mass fractions near interfaces are continuous.

Solution Initialization and Iteration

Again, the solution must be initialized so that FLUENT has initial values for its first iteration. This is similar to the periodic run, except that additional values have to be specified. The mass fraction for each

species has to be initialized, and the user defined scalars have to be initialized as well. These are initialized with the values for the mass fractions given above in Table 6.

The solution could not be iterated at this point though. The methane would get rapidly depleted over a few iterations and go into the negative. When the user defined function then attempts to take the square root of that negative value, an error occurs. In order to prevent this, two methods were used. At first a bootstrapping procedure was utilized in which the solid density was lowered in the C file, which effectively lowered all reaction rates since they are all multiplied by the solid density. The density used was 1% of the initial value. After several hundred iterations were run successfully, the density was changed to 10% of the actual value. Then after several hundred iterations the solid density was changed back to its actual value of 1947 kg/m^3. This proved to be a tedious process and was prone to failure. Over the course of this project a more effective method was utilized. The relaxation factors for the user defined scalars under the solution controls in FLUENT were changed to 0.5. This means that after each iteration the user defined scalars only changed by 50% of the change that FLUENT would normally apply. This prevented the user defined scalars from dropping into the negative and made for smooth FLUENT runs.

Convergence

Residuals do not give a valid measure of solution convergence in the reaction case. The user defined scalars still change significantly after the residuals have stopped changing due to the complexity of the case with the user defined functions. Therefore, a surface monitor was defined. The user defined scalar 1, which represents hydrogen mass fraction, was defined as an integral surface monitor over all surfaces of the test particle. The plots for this surface monitor can be found in Appendix A. The solution was usually converged after 15,000-20,000 iterations. The reaction cases were run on multiple parallel processors to speed up the iterations.

Post-processing

Once the reaction case was converged, the various post-processing features of FLUENT were utilized. These including plotted contours of velocities and species concentrations as well as flow path-lines and temperature distributions.

CHAPTER 4: RESULTS AND DISCUSSION

4.1: Numerical Results

After the solutions for each of the nine reactor segment models were converged (refer to Appendix A), a wide range of results were collected. These were separated into purely numerical results obtained from FLUENT and graphical interpretations of results displayed on the model itself. Numerical results are discussed first. All results for the 4H and 4HG models were obtained by solving previously developed FLUENT case files by Boudreau and Rocheleau on the basis of a fixed mass flow instead of a fixed pressure drop [3]. The same is true for the 5HP geometry, which was created previously by Carr and solved on the basis of constant pressure drop as well [4]. The results for the 6 other catalyst geometries are based on purely original work.

4.1.1: Wall Segment Results

Numerical results were collected in FLUENT using its various post-processing features as well as user defined functions. The numerical results pertinent to the wall segment are presented in Table 7.

Table 7: Wall segment results

Shape	Average Reactor Wall Temperature (K)	Pressure Drop (Pa/m)	Void Fraction	Average Outlet Temperature (K)
4H	1090.2	1973.7	0.66414	828.33
4HG	1104.2	1627.8	0.71964	828.85
4HD	1146.6	651.2	0.74497	829.34
4HGD	1120.3	652.4	0.78074	828.83
5HP	1103.3	1612.6	0.77333	829.05
5BHPD	1043.2	649.8	0.82694	828.37
5HPD	1095.2	1486.0	0.72716	829.61
6HG	1102.0	1712.2	0.74026	828.27
6HGD	1117.4	618.2	0.79631	828.14

All averages are area-weighted averages, meaning a surface integral was performed over the appropriate surface and the result was then divided by the total surface area to yield the average. The first trend that can be identified is increasing average wall temperature with increasing void fraction. To visualize this trend, the average reactor wall temperature was plotted against the void fraction of the corresponding geometry. A linear fit was applied to the data set and an R-squared value of 0.7373 was obtained, as shown in Figure 8. The trend line was only applied to the 7 data points marked in blue.

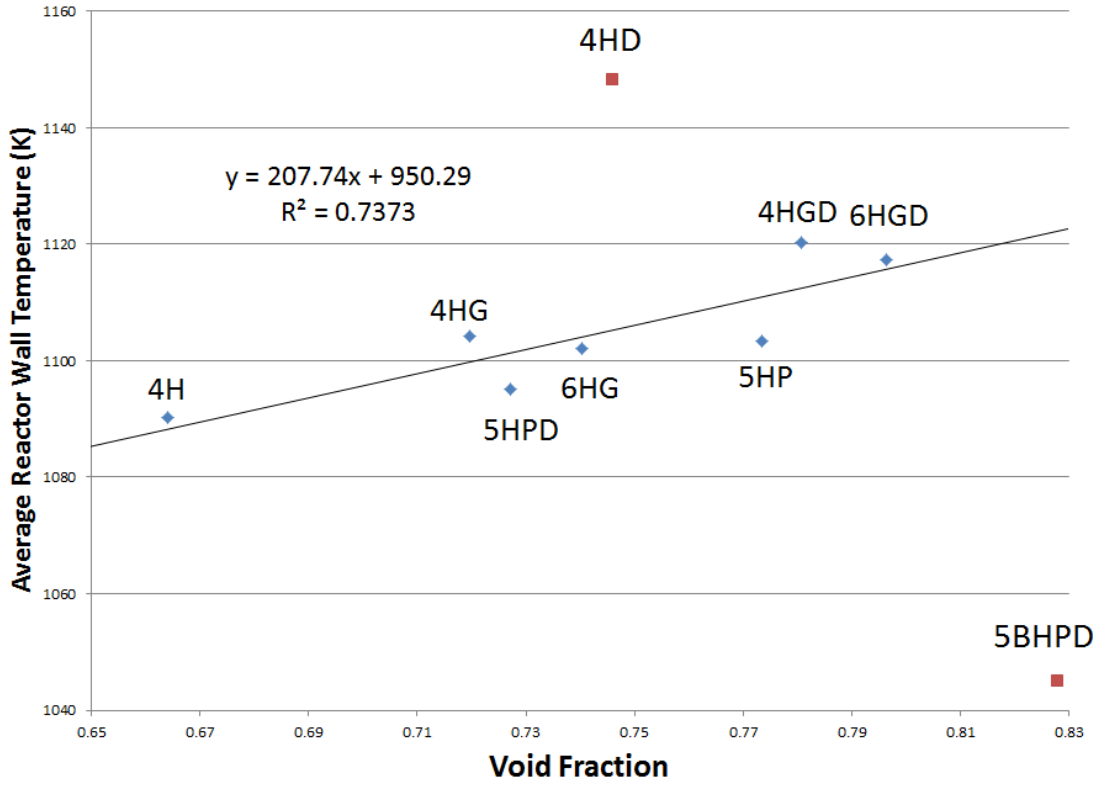

Figure 8: Reactor wall temperature versus void fraction for the geometries studied

It can be seen that the trend line fits the blue data set well and a correlation exists. The R-squared value of 0.7373 can be interpreted as 73.73 % of the variation in wall temperature being explained by the variation in void fraction. This is to be expected, since adding various features to the catalyst geometries usually has the result of less radial flow. For example, it can be seen that out of the 4H and 4HG shapes, the 4HG geometry had the higher wall temperature. This can be explained by the grooves of the 4HG shape which tend to guide fluid flow along the length of the catalyst. This reduces the scattering of fluid in the radial direction and reduces heat transfer from the reactor wall to the fluid. As a result, the

average reactor wall temperature was higher than for the 4H case. The 4HD case had the highest wall temperature out of all geometries studied and was an outlier not considered in the linear regression. This can be explained by its domed ends, which create smooth, rounded surfaces over which fluid can easily flow. The 4HD shape was the only geometry studied that only had domed ends as its features and no grooves. Without grooves, the fluid flow over the outside surface of the catalyst was undisturbed and could easily flow around the catalyst and continue in the z-direction. This makes for a significantly low radial flow. Additionally, the 4HD case has the lowest number of holes, which means that less fluid volume travelled through these holes. Since catalyst geometries are generally packed at angles in the tube, as shown previously in Figure 4, flow through catalyst holes change the direction of fluid flow into the radial direction. Therefore less radial flow occurred in the 4HD model and its wall temperature is significantly higher than all other shapes. It should also be considered that the domed catalysts had a smaller volume than those without domes, their positions in the wall segment, however, did not change. This created artificially large gaps between catalysts, enabling fluid to flow in the z-direction relatively undisturbed.

When comparing the 5 and 6-holed cases, the same trend of increasing wall temperature with increasing void fraction can be observed, for the same reasons as the four-holed geometries. The exception to this is the 5BHPD case, which has the highest void fraction but the lowest wall temperature out of all catalysts studied and is the second outlier of Figure 8. This can be explained by the 5 holes of this shape, which change fluid flow towards the radial direction, as mentioned earlier. The 5BHPD catalyst has larger hole diameters than the 6-holed shapes and the 5HPD geometry. Additionally, its domed shape increases the distance between the particle and the tube wall, allowing for a larger volume of fluid to travel between the wall and the catalyst. This makes for more efficient convective heat transfer. Combined with its 5 holes with large diameters, the 5BHPD shape was ideal for radial heat transfer.

Another trend that can be identified is decreasing pressure drop with increasing void fraction. This is to be expected, since an increased void fraction means the volume of fluid in the wall segment is higher. Since the mass flow rate was held constant in this study, mass conservation principles can be used to reason that the fluid velocity was therefore lower. Since a lower velocity means a lower pressure drop, decreased void fractions of the catalyst beds resulted in higher pressure drops. Void fraction can also be related to the average outlet temperature. The outlet temperature of the gas remained fairly constant in this study and varied only one degree Kelvin, but a trend can still be identified. As void fractions

increase, the average outlet temperature of the gas is lower. The same explanation as for the average reactor wall temperature is valid. A larger void fraction general means less radial flow and less radial heat transfer, therefore less heat was transferred to the gas before it exits, decreasing its temperature. This, however, is balanced by the longer residence time of the gas in the wall segment, hence the small variations in outlet temperature.

4.1.2: Test Particle Results

Next, the numerical results for the test particle are considered. These are shown in Table 8 below.

Table 8: Test particle results

Shape	GSA (m^2)	Heat Sink (W)	Surface Heat Flux (W)	Avg. Temp. Particle (K)	CH4 Consump. (kmol/s)	H2 Production (kmol/s)	CO Production (kmol/s)	CO2 Production (kmol/s)
4H	5.03E-03	61.125	61.145	800.72	-3.64E-07	1.43E-06	2.59E-08	3.38E-07
4HG	5.20E-03	61.297	61.362	799.90	-3.65E-07	1.43E-06	2.56E-08	3.39E-07
4HD	4.02E-03	44.346	43.499	795.93	-2.67E-07	1.05E-06	1.75E-08	2.49E-07
4HGD	4.15E-03	43.977	43.991	794.89	-2.62E-07	1.03E-06	1.68E-08	2.46E-07
5HP	5.74E-03	61.136	61.162	801.81	-3.64E-07	1.43E-06	2.65E-08	3.37E-07
5BHPD	4.61E-03	50.132	50.147	797.24	-2.99E-07	1.17E-06	2.05E-08	2.78E-07
5HPD	4.12E-03	44.600	44.590	797.35	-2.66E-07	1.04E-06	1.87E-08	2.47E-07
6HG	5.81E-03	63.253	63.245	801.98	-3.76E-07	1.48E-06	2.75E-08	3.49E-07
6HGD	4.67E-03	50.903	50.863	797.58	-3.03E-07	1.19E-06	2.16E-08	2.82E-07

It can be seen that the geometric surface area (GSA) of domed catalysts is lower than those of the other catalysts, since the domed ends reduce the surface area at the edges of the cylinders. It should be kept in mind that the domed ends also decrease the space that the pellets occupy in the reactor tube. This means that the catalysts would pack closer and more catalysts can fit into the reactor tube, which in turn would mean a higher total catalyst surface area. Since the positions of catalysts did not vary in this study, however, this does not occur for the systems modeled.

The heat sink of the catalysts is the amount of energy that the reaction consumed on and inside the catalyst and was calculated by a user defined function. The total surface heat fluxes for the geometries were calculated natively by FLUENT by performing an energy balance. The two results should be equal to each other and can be compared as a measure of solution convergence. It is seen that the two values are in good agreement for each shape. The heat sink is also an indicator of reaction rate, since a higher reaction rate means a higher heat sink for the particle due to the endothermic nature of the reaction kinetics. It can be seen that there is little variation between the catalysts without domes; the heat sinks remain fairly constant at 61W with the 6HG shape being the exception. The 6HG geometry had the largest heat sink, which makes sense since it also had the highest GSA.

As mentioned earlier, the reaction is strongly diffusion-limited. This means most of the reaction occurs on the surface of the catalysts. Therefore a higher GSA leads to a higher total heat sink for the particle. This same relationship exists for the species production and consumption rates. More methane is consumed, and more hydrogen, carbon monoxide, and carbon monoxide was produced if the catalyst had a higher GSA and therefore a higher heat sink. The average particle temperature was the lowest for the 4-holed shapes with domes and the highest for the 5 and 6-holed geometries without domes. The same analysis as previously for the average reactor wall temperatures can be applied to this phenomenon. Less radial heat transfer means less heat is transferred to the particle, resulting in a lower particle temperature. Since domed shapes decrease radial heat transfer, these particles had the lowest average temperature.

As noted previously, the domed catalysts studied had a significantly lower volume than those catalysts without domes. Therefore, the domed catalysts had lower heat sinks and lower species production and consumption rates. This appears to give the impression that domed catalysts are not suitable in SMR due to their low reaction rates. However, the particles would pack closer in the reactor tube, making for a higher number of catalysts for a given reactor tube volume. This, in turn, means that there would be more catalysts and therefore a higher surface area and higher reaction rates. To compare catalyst geometries on an equal basis, the total reaction rates for each test particle was divided by its volume. The results are shown in the form of a bar graph in Figure 9.

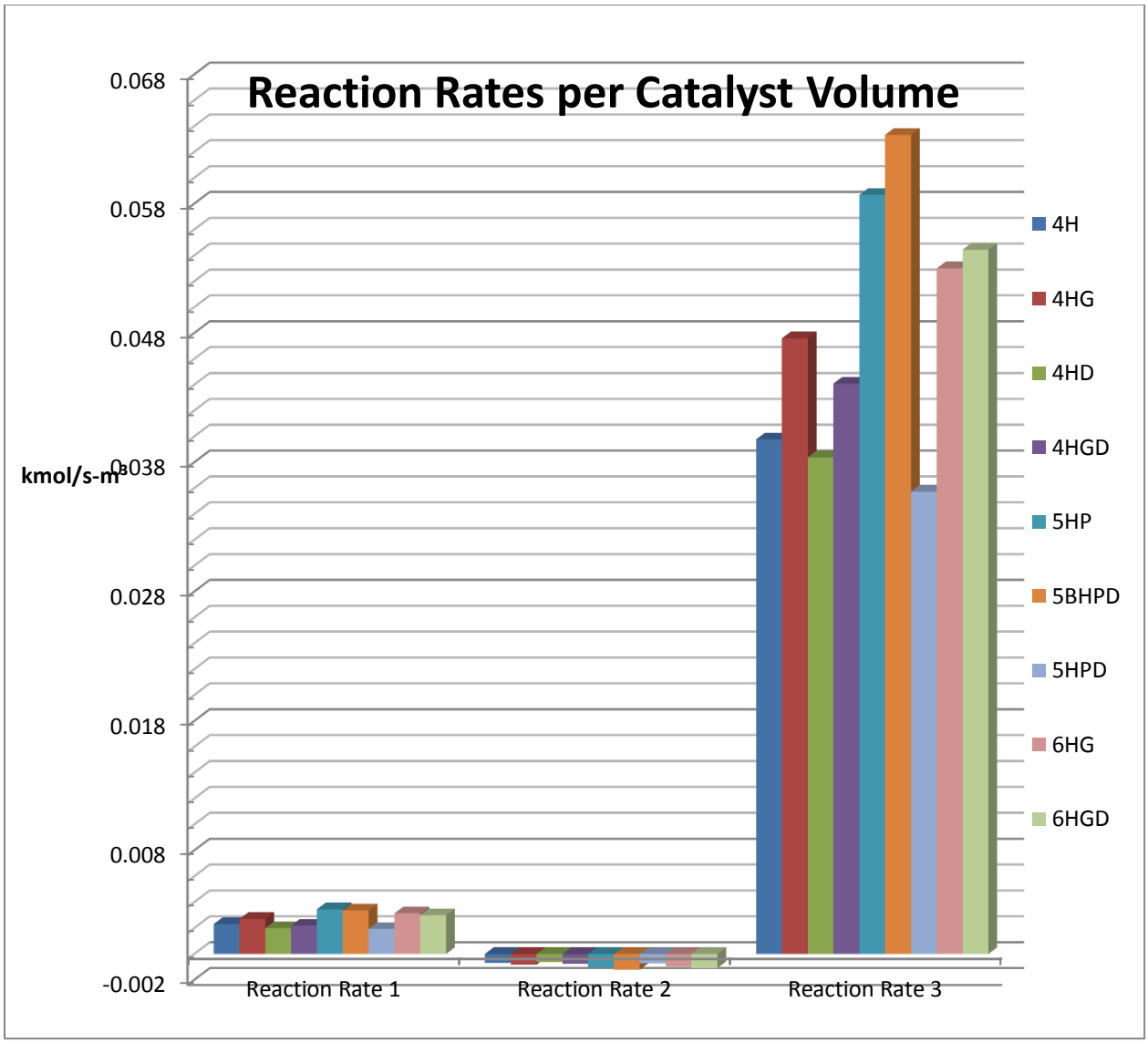

Figure 9: Test particle reaction rates

It is easy to identify the fact that the third reaction proceeds the most rapidly out of the three reactions. It produces four moles of hydrogen gas for each mole of methane reacted, more than any of the other two reactions (see Table 1). Since reaction three produces the most moles of hydrogen and has the highest reaction rates, it is also the most important to analyze. It can be seen that the two 5-holed geometries with the large diameter holes, the 5HP and the 5BHPD geometries, have the highest reaction rates per catalyst volume. This makes sense since the 5 wide holes decrease the catalyst volume while at the same time providing surface area for the reaction to occur. Heat transfer also plays a role, since the endothermic reaction kinetics need thermal energy to proceed. As previously described, the 5HP and

5BHPD cases exhibited good radial heat transfer with low reactor wall temperatures. Therefore they had relatively high reactions rates combined with low catalyst volumes. The shapes with the second-highest reaction rates per volume were the 6HG and 6HGD geometries. The 6HG geometry has good radial heat transfer and the highest GSA. Therefore it has high reaction rates, even when divided by its large volume. The 6HGD shape has much of those same characteristics but a lower catalyst volume, hence its higher reaction rate per volume than the 6HG case. The 4-holed catalysts did not perform well in this comparison due to their lower surface areas and lower void fractions.

4.2: Graphical Results

A large number of results were collected in graphical form. These include temperature and reaction rate contours as well as methane and hydrogen mass fractions contours. Fluid pathlines are also presented and an iso-surface of constant height as well as a line through the reactor was created to analyze reactor results.

4.2.1: Contours of Temperature on Test Particle

First, temperature contours are analyzed. Temperature contours were plotted on the surface of each test particle and are displayed in Figure 10 below.

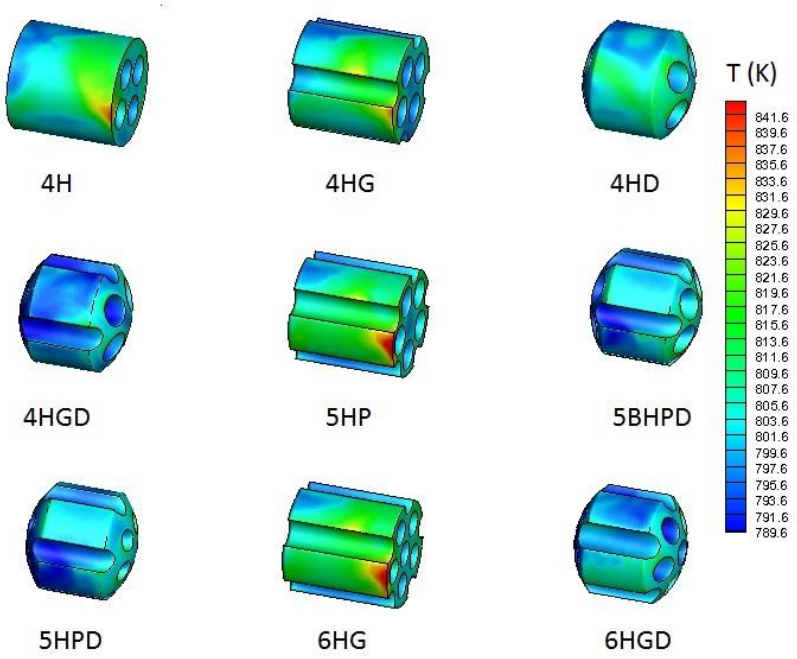

Figure 10: Test particle temperature contours

The color scale was held constant for each catalyst and varied from 790 K to 842 K. There are several patterns that can be identified. First, all catalyst shapes that did not have domes had small regions of high temperatures, or a hot spot. The fact that domed shapes did not have a hot spot is believed to be a flaw of the model. Since the positions of the catalysts did not change, the domed ends removed much of volume of the catalyst ends, therefore creating artificially large gaps between the catalyst and the wall. In reality, these domed catalysts would be closer to the reactor wall and it is likely that a hot spot would develop for these domed geometries as well. It can also be seen that as the void fraction increases, the hot spot becomes more intense for each test particle. This can be explained by the larger volume of fluid with higher void fractions, making for more efficient convective heat transfer.

4.2.2: Contours of Temperature and Velocity on Iso-Surface

A surface was defined of constant height in the reactor tube to analyze the cross-sectional temperature and velocity contours in the reactor tube. The surface was defined at a z-coordinate of 0.020876214 m and its location relative to the wall segment model is presented in Figure 11 below. The model displayed is the 5BHPD geometry, and contours of temperature are shown.

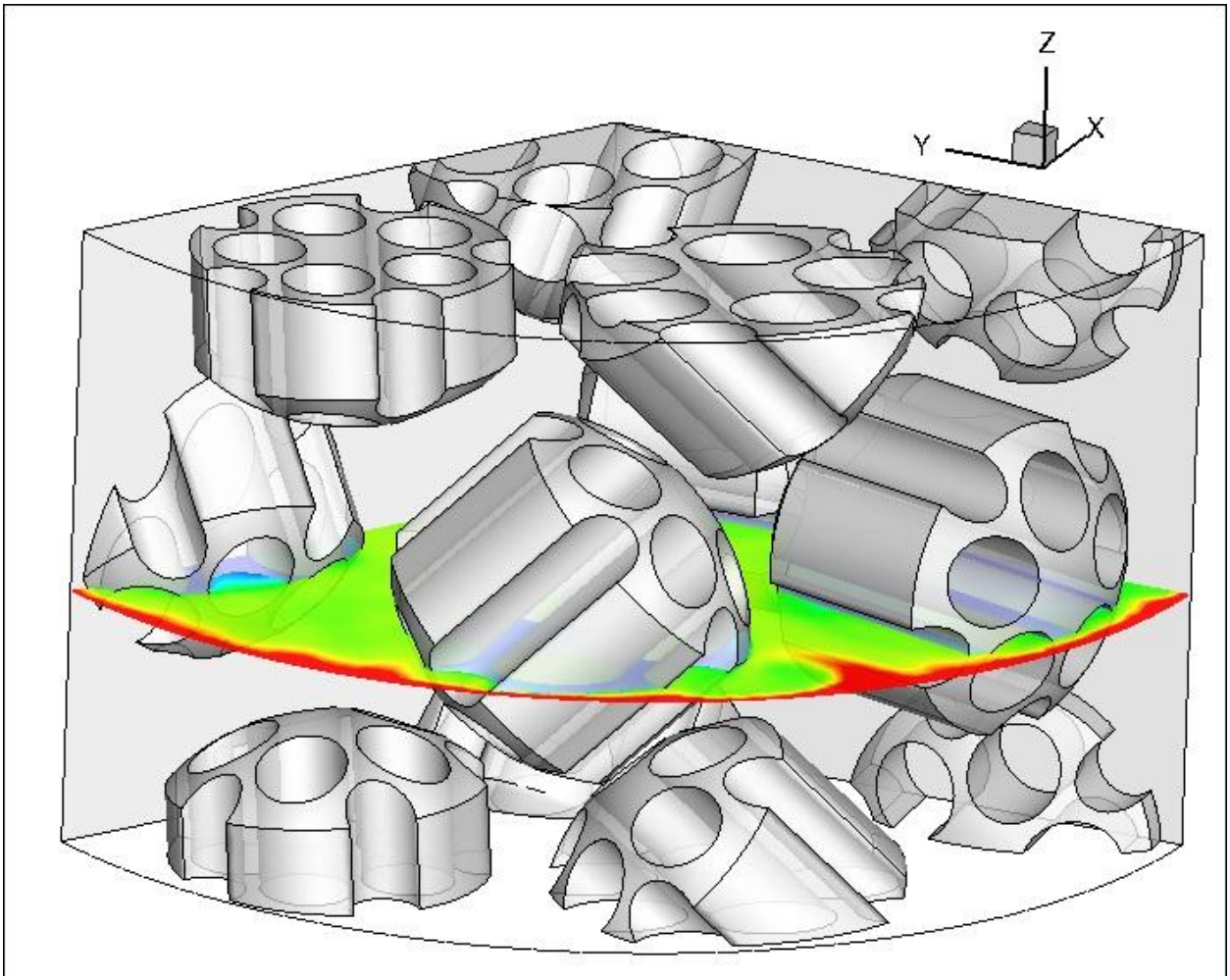

Figure 11: Location of iso-surface, 5BHPD geometry shown

The height of the iso-surface was chosen so that it would intersect the test particle precisely at the location of the hotspot for those geometries that had such a hot spot. The temperature and velocity contours on the iso-surface for the 4-holed geometries were considered first and are displayed in Figure 12 below, with temperature contours on the left and velocity contours on the right.

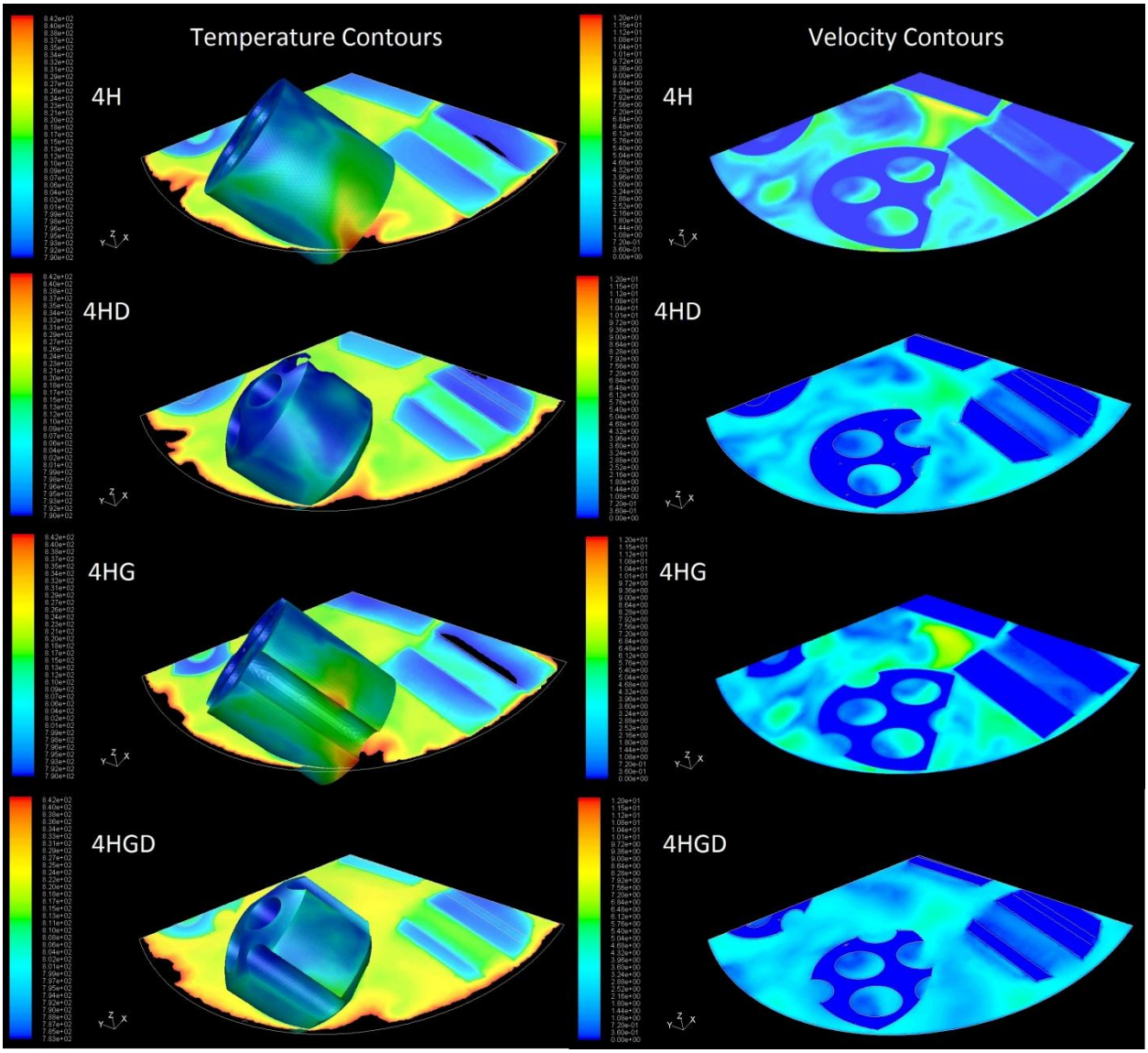

Figure 12: Temperature and velocity contours for 4-holed catalysts

Temperature contours are displayed not only on the iso-surface, but also on the surface of the test particle to aid in the analysis of the hot spot. It can be seen that the hotspot is interrupted for the 4HG case by the groove running along the length of the pellet. Therefore two hot spots are visible, one on each side of the groove, directly above each other. As shown before, the 4HD and 4HGD geometries do not have hotspot. The iso-surface allows for the confirmation of the earlier assumption that the domed shape created larger separation between the particle and the reactor wall. Towards the right of the test particle is another solid catalyst in the tube. When comparing the location of this particle for the four cases, it can be seen that for the geometries with domed ends there is a much larger separation

between the reactor wall and the particle. The same is true for the test particle, and this is what prevents the domed catalysts from having hot spots. From the velocity contours, it can be seen that the region of high velocity near the center of the wall segment decreases in intensity as void fraction increases, as expected. Next, temperature and velocity contours for the 5 and 6-holed geometries are presented in Figure 13 below.

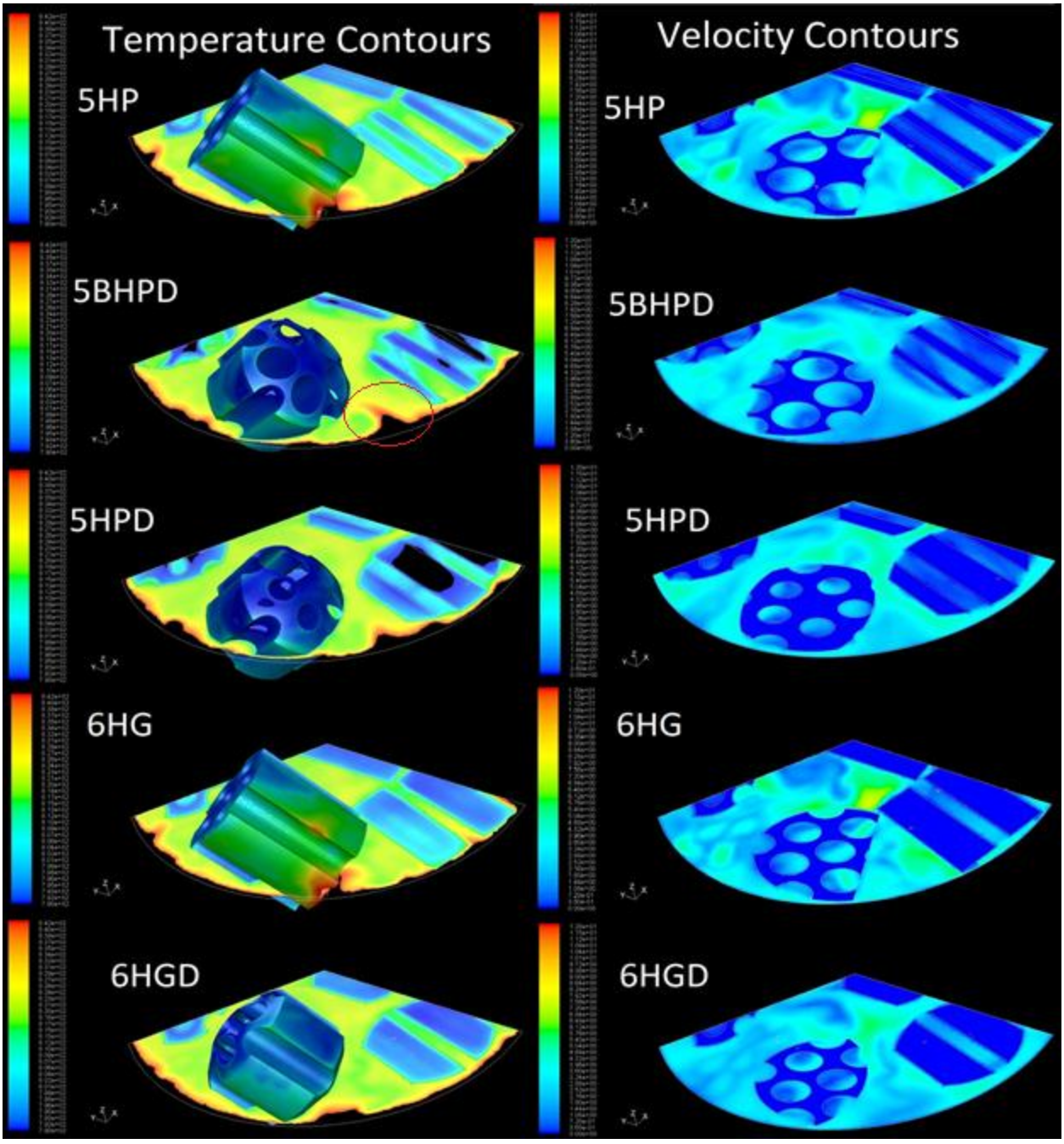

Figure 13: Temperature and velocity contours for 5 and 6-holed catalysts

The range of temperatures for the temperature contours was kept equal to that of the previous figure, therefore some black spots exist on the iso-surface and the test-particle has some invisible sections where the temperature was lower than the minimum temperature in the color band. This is aesthetically unpleasant but makes for a more effective comparison. For the 5 and 6-holed cases, much of the same trends as for the 4-holed geometries can be identified. Domed geometries did not exhibit a hot spot due to their increased separation for the reactor tube wall. Test particle temperatures are generally lower for domed geometries due to their decreased radial heat transfer. As before, two locations of the hot spot are identified on each catalyst with grooves and no domes since the groove running along the length of the catalyst cuts through the location of the hot spot. A significant detail present in one of the temperature contours should be noted. For the 5BHPD case, there is a tongue of high temperature that is going towards the fluid in the reactor tube between the test particle and the catalyst next to it. It is circled in red on the figure. This is indicative of good radial heat transfer and explains the low reactor tube wall temperature for the 5BHPD configuration. The velocity contours are again related to void fraction. The regions of high velocities are more intense for geometries with lower void fractions.

4.2.3: Contours of Species Mass Fractions

Contours of mass fractions for methane and hydrogen are displayed on each test particle in Figure 14 below. In FLUENT, methane mass fractions were represented by the user defined scalar 0 (UDS0) and hydrogen mass fractions were represented by the user defined scalar 1 (UDS1). Contours of methane mass fractions are shown on the left, and those of hydrogen mass fractions are displayed on the right.

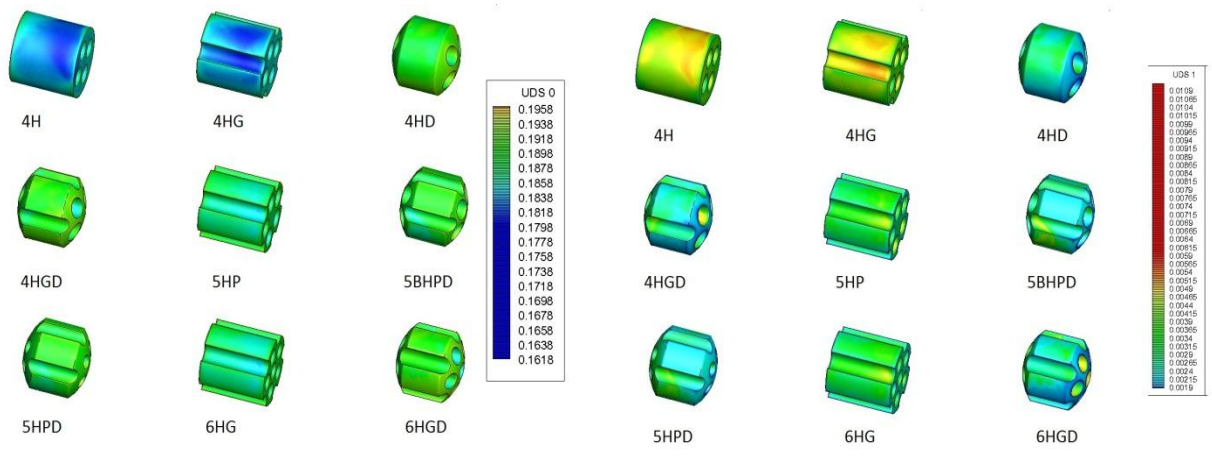

Figure 14: Contours of methane and hydrogen mass fractions

It can be seen that where areas of low methane mass fraction exists, there are corresponding areas of high hydrogen mass fractions for each catalyst geometry. This is expected since methane is consumed in the SMR reaction mechanism, therefore low concentrations of methane mean that this methane has been reacted and hydrogen has formed in these areas. It can be seen that the locations of the hot spots presented earlier generally correspond to areas of high hydrogen mass fractions. For all grooved catalysts without domes, this area of high hydrogen mass fractions exists in the groove that intersects the hot spot, as presented earlier. Another trend that can be seen is that catalysts without grooves have higher methane conversion and hydrogen production on their outside surfaces. The 4H and 4HD configurations both have higher hydrogen mass fractions and lower methane mass fractions than their corresponding grooved geometries (4HG and 4HGD).

4.2.4: Velocity-Colored Pathlines

Velocity-colored pathlines for the 4H, 4HD, 4HG, and 4HGD catalyst geometries are displayed in Figure 15 below. The velocity color-band ranged from 0 to 12 m/s for all shapes.

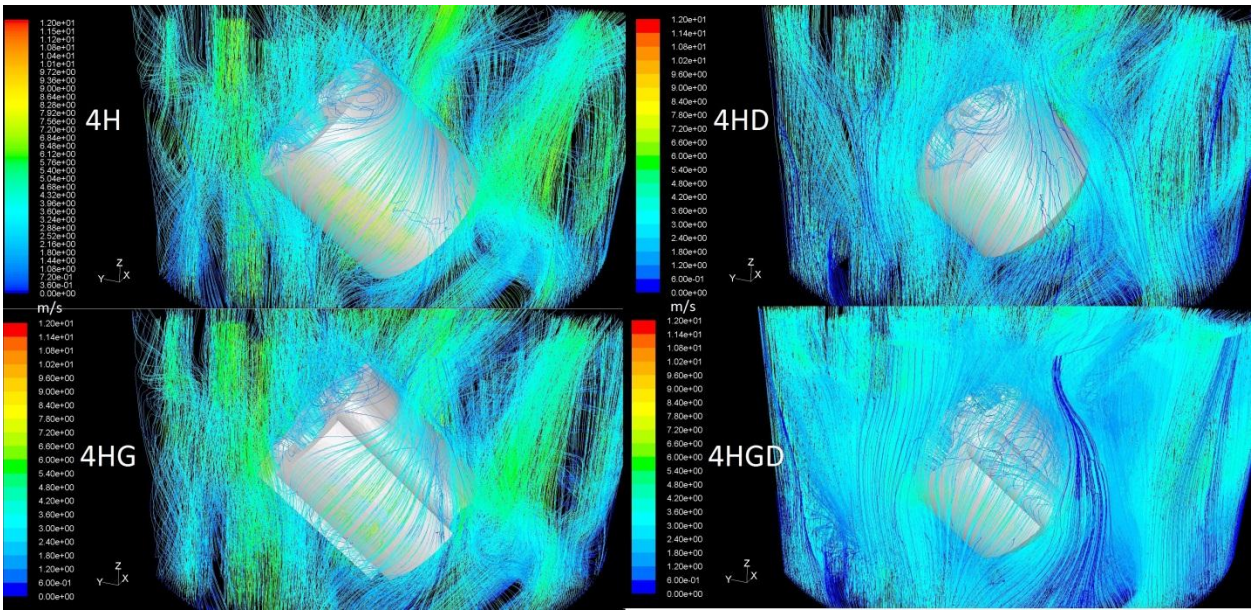

Figure 15: Velocity-colored pathlines for 4-holed catalysts

The pathlines reveal the fluid behavior for catalyst shapes with domed ends and for those without domed ends. It can be seen that for the 4H and 4HG shapes which do not have domed ends, there is high-velocity flow in the radial direction and the fluid scatters off the edges of the catalyst ends. It can also be seen that fluid flow over the outside surface of the 4H and 4HG shapes is normal to the direction

vector of the test particle, further increasing radial mixing and heat transfer. This fluid behavior is not seen in the 4-holed configurations that have domed ends, the 4HD and the 4HGD shapes. Fluid flow is primarily in the z-axis direction, with no corners or edges that could disrupt its flow. The pathlines hug the smooth, aerodynamic outside surface of the domed catalysts and do not scatter. This explains the lower radial heat transfer rate in those configurations as well as their lower pressure drop. It can also be seen that fluid velocity for the domed catalysts is lower than that of the 4H and 4HG catalysts, were the fluid velocity is high and scattered.

The fluid pathlines for the remaining geometries, the 5 and 6-holed configurations, are displayed below in Figure 16. Pathlines are again colored by velocity ranging from 0-12 m/s.

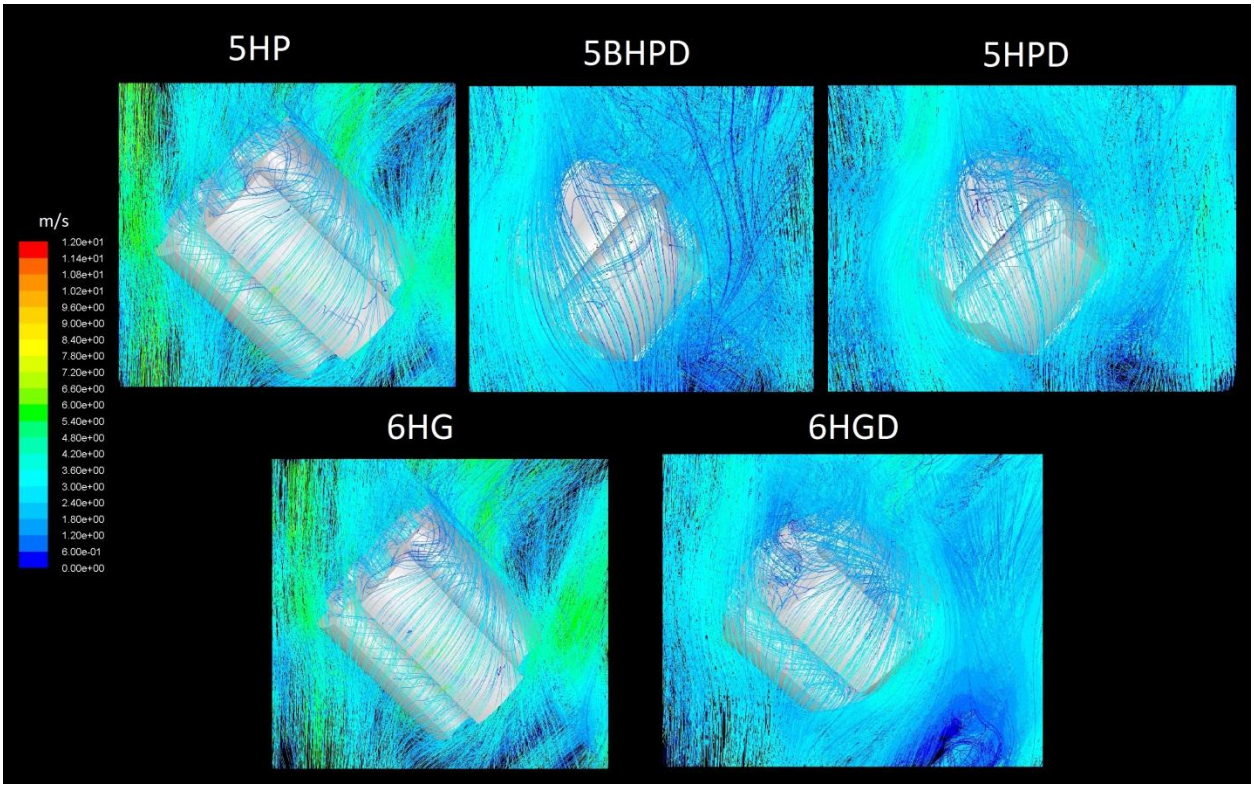

Figure 16: Velocity-colored pathlines for 5 and 6-holed catalysts

The fluid behavior for the 5 and 6-holed configurations is very similar to the 4-holed geometries. Catalysts without domes have fluid flow over their outside surfaces normal to the direction vector of the test particle. The edges and corners make for scattered fluid flow and increase radial mixing. Domed catalyst shapes have fluid flow that hugs their outsides surfaces and fluid flow is primarily in the z-coordinate direction with little radial flow. Velocities are lower for domed shapes since their void

fractions are higher. It can also be seen that the 5BHPD geometry has more radial mixing than the 5HPD case. This can be explained by the larger diameter holes of the 5BHPD shape which redirect fluid flow towards the radial direction. It also seems that the lower fluid velocity for the 5BHPD shape prevents the fluid exiting its holes from being forced to flow into the z direction by the fluid flow over its outside surface. This is evident in the 5HPD case with smaller diameter holes. The high velocity and large volume of flow over its outside surface redirects the small flowrate of fluid through its holes to the z direction. As a result, radial heat transfer is significantly better for the 5BHPD case, even though the configuration of the 5HPD shape is very similar.

4.2.5: Radial Temperature Profile

A line was created in the post-processing phase in FLUENT that runs through the radial width of the wall segment. Its two endpoints have coordinates of (-0.0478172, -0.0171106, 0.0256169) and (-0.000226916, -0.00115509, 0.0230392), where the former is at the reactor wall and the latter is close to its center. The line is just above the height of the iso-surface defined earlier and is depicted in Figure 17 for the 5BHPD geometry.

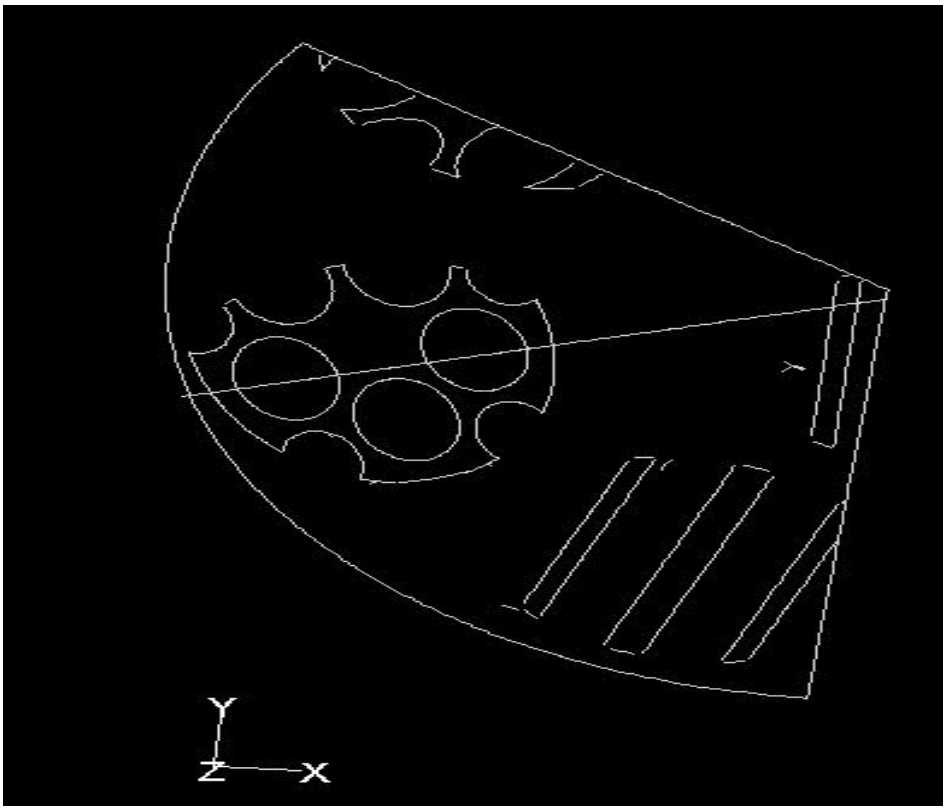

Figure 17: Location of the line in respect to the iso-surface

The line starts at the reactor wall and cuts through the test particle. It then intersects the fluid space and ends near the center of the wall segment. It was of interest to plot the temperature profiles for the various geometries studied in order to compare their radial heat transfer rates. The temperature profiles for the 4-holed configurations are shown in Figure 18, where temperature is plotted against the x-coordinate.

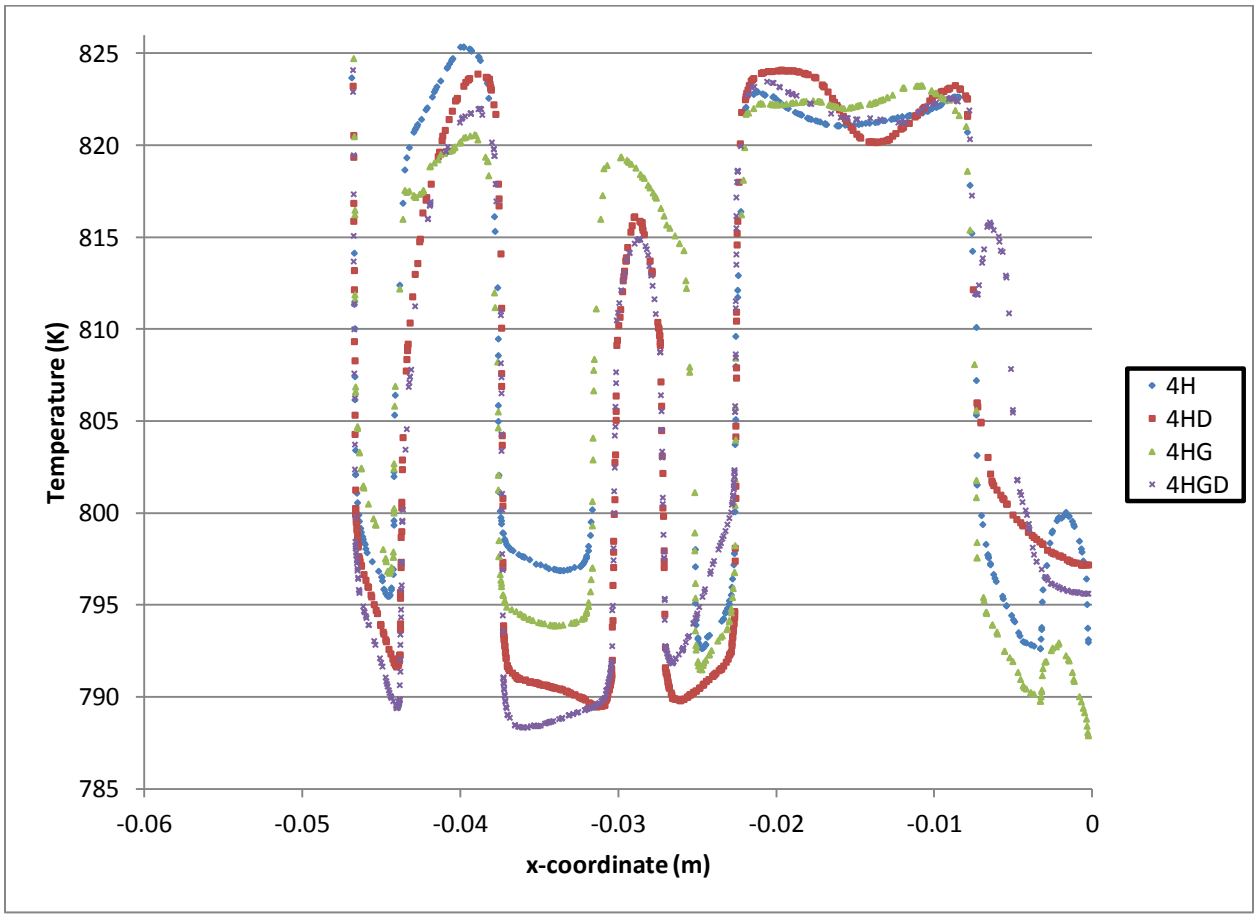

Figure 18: Temperature profile for 4-holed catalysts

In Figure 18, it is convenient to analyze solid temperatures since the temperatures for the fluid sections are quite similar to each other. The x-coordinate range -0.04 to -0.03 represents the location of the solid test particle. It can be seen that the 4HGD and the 4HD catalyst geometries resulted in the lowest solid temperature. This agrees with results from earlier sections where it was determined that geometries with domed ends generally have lower radial heat transfer rates. Lower radial heat transfer means that less heat was transferred from the reactor wall to the fluid, and then from the fluid to the solid catalyst. The 4H geometry had the highest solid temperature, and the temperature of the 4HG shape was about 5

K lower. This makes sense since the 4H geometry has the most fluid scattering and radial heat transfer out of the 4-holed geometries, as shown by the pathlines in Figure 15. The grooves funnel flow along the length of the catalyst, reducing radial heat transfer. Therefore the 4HG solid temperature was lower than that of the 4H case.

The temperature profiles for the 5 and 6-holed geometries are depicted in Figure 19 below.

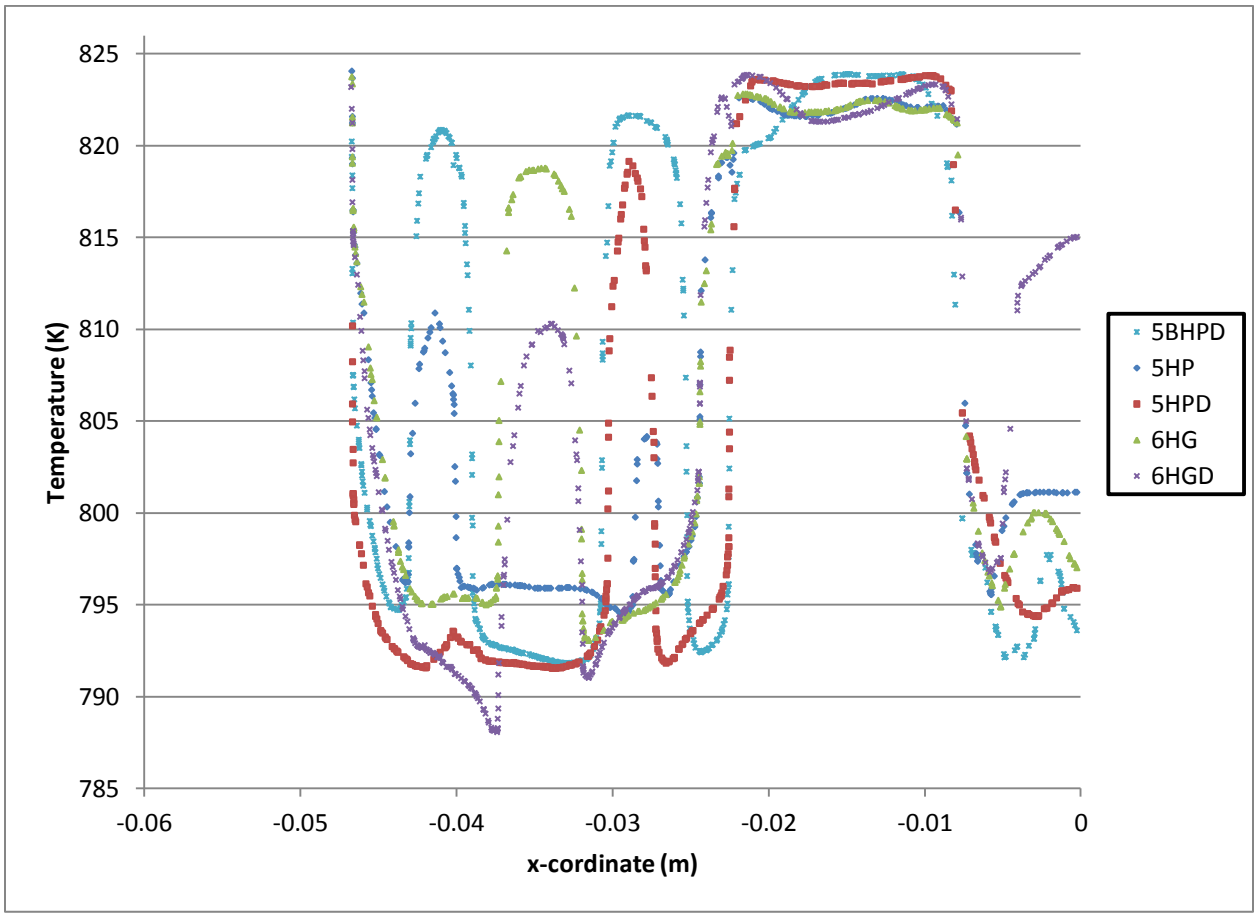

Figure 19: Temperature profile for 5 and 6-holed catalysts

Examination of the 5 and 6-holed temperature profiles leads to the conclusion that the 5BHPD geometry is superior to all other shapes in terms of radial heat transfer. Its fluid temperature is consistently higher than that of other catalysts. It even has better heat transfer properties than the 5HP geometry. For example the 5BHPD's fluid temperature is more than 10 K warmer than that of the 5HP shape near the x-coordinate of -0.04. As expected, the 6HG shape had better heat transfer properties than the 6HGD geometry, since its fluid temperature was higher. This can easily be seen near the x-coordinate of -0.035 where the 6HG fluid temperature is about 8 K higher than that of the 6HGD shape.

4.2.6: Contours of Reaction Rates

Contours of reaction rates were plotted for the 5BHPD and 6HG geometries. These were plotted on the iso-surface that was defined in previous sections. Only the surfaces of the test particles are shown to aid in direct comparison between the two geometries. The 6HG and 5BHPD shapes were chosen because the 6HG configuration had the highest total reaction rates and the 5BHPD shape had the highest reaction rate per catalyst volume. The contours for reaction rates for reaction 1 and reaction 3 are displayed in Figure 20 below.

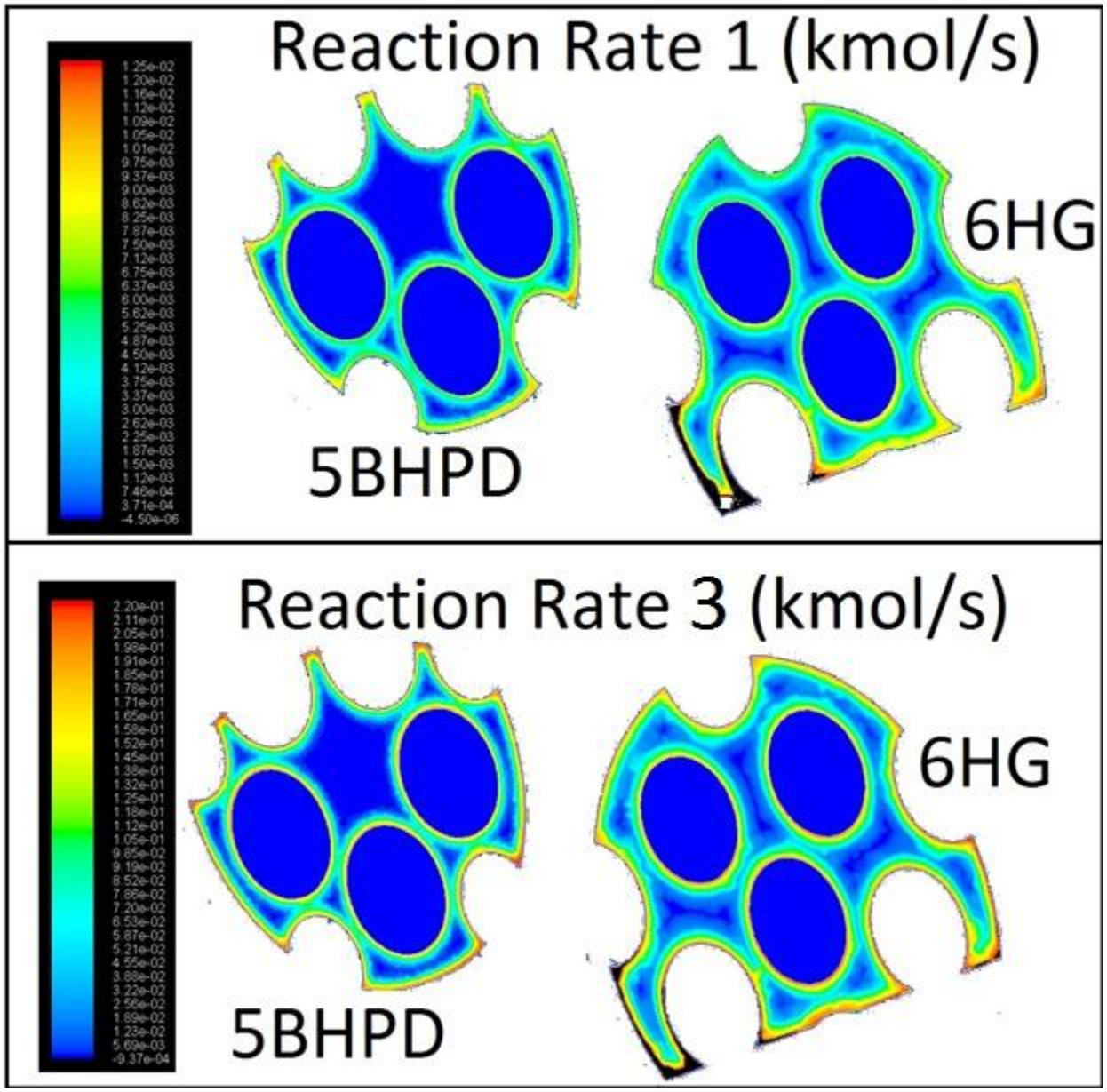

Figure 20: Reaction rate contours for 5BHPD and 6HG geometries

From the figure, it is seen that the reactions takes place primarily on the outside surface of the catalyst, as expected. This confirms the assumption that the reaction is strongly diffusion-limited and the reaction sites in the interior volume of the catalysts are not utilized. Therefore a high surface area to volume ratio is desirable in SMR. This also explains why the 5BHPD geometry performs much better than the 5HPD shape, which had the same catalyst features but a narrower hole diameter. Narrower holes means that the surface area is reduced and less reaction sites are available on the surface of the catalyst. It also means that more unused reaction sites exist in the interior of the catalyst.

It can also be concluded that hot spots result in high reaction rates in those concentrated regions of high temperatures. In Figure 20, any areas colored in black represent areas of reaction rates that exceeded the maximum value of the color band. Knowing this, it can be seen that for the 6HG geometry the black region of high reaction rate directly corresponds to its hot spot identified earlier in this paper.

CHAPTER 5: CONCLUSIONS AND RECOMMENDATIONS

Steam methane reforming (SMR) is a process used commonly in the industry to convert methane into syngas, which is a mixture of hydrogen, carbon dioxide, and carbon monoxide. It is the cheapest method to produce hydrogen to date and is used in many applications, ranging from producing hydrogen for fuel cells to manufacturing hydrogen in the synthesis of ammonia. A typical steam reformer is made up of many long, narrow reactor tubes packed with catalyst pellets. These pellets vary in shape and size and affect the process properties. SMR reaction kinetics are endothermic, therefore reactor tubes are externally heated to increase reaction rates.

The goals of this project were to identify favorable catalyst design features as well as to recommend the most suitable catalyst in SMR to be used in the industry. These goals were realized by utilizing Computational Fluid Dynamics (CFD) to analyze a 120^{o} wall section of a reactor tube. Nine different catalyst geometries were studied, all were cylindrical in shape and had various features such as holes, grooves, and domed ends. Three of these were previously studied, and the number of holes ranged from 4 to 6.

First, the results for the wall segment as a whole were studied. Several trends of catalyst design features were identified. Increasing void fraction of the wall segment led to increased average wall temperatures. More specifically, grooves along the length of the catalyst tend to guide fluid along the length of the catalyst and reduce radial flow and heat transfer. Domed ends create smooth, rounded surfaces over which fluid flows without scattering, which again leads to less radial flow and heat transfer. The 5BHPD geometry, however, was an exception to this and had the lowest wall temperature out of all catalysts studied. This was explained by its 5 wide holes which redirect flow into the radial direction combined with its larger fluid volume between the catalyst and the reactor wall caused by its domed ends. It was also shown that increasing void fraction led to a lower pressure drop in the system; the 6HGD shape had a pressure drop of 618.2 Pa/m and the 5BHPD geometry had a slightly higher pressure drop of 649.8 Pa/m. The 6HG geometry, on the other hand, had a high pressure drop of 1712.2 Pa/m.

The results for the test catalysts were studied next. Geometric surface area (GSA) of the catalysts with domed ends was lower, but it was reasoned that domed catalysts would pack closer in the reactor tube

since they had lower volumes than the other geometries. It was found that heat sinks for catalysts without domes were relatively equal at 61W with the exception of the 6HG which had a heat sink of 63.2 W. The 6HG geometry had the largest geometric surface area and the highest reaction rates. However, this seemed like an unfair comparison since the model did not take into account the denser packing that domed catalysts would exhibit. Therefore reaction rates per catalyst volume were considered. It was found that the 5BHPD geometry had the highest reaction rates per volume, with the 5HP geometry close behind.

Therefore it was concluded that both grooves and domed ends decrease pressure drop but tend to increase reactor wall temperatures. It is also concluded that wider diameter holes are favorable since they decrease pressure drop and encourage radial flow and radial heat transfer. The 5HP and 5BHPD geometries offered the ideal number and diameter of holes, with low tube wall temperatures and low pressure drops when compared to similar 6 and 4-holed geometries. Overall, it was determined that the 5BHPD geometry, which consists of 5 wide holes, 5 grooves and domed ends, had the most favorable characteristics and is recommended to be used as the packing pellets in steam reformers. It had a low pressure drop and high reaction rates per volume. It also exhibited excellent radial mixing and radial heat transfer that resulted in high fluid temperatures and the lowest tube wall temperature out of all geometries studied. Good radial heat transfer reduces thermal stresses on the system and increases its life span, which will save manufacturers money. High fluid temperatures result in the high transfer of thermal energy to catalysts. This leads to high reaction rates and a high conversion of methane.

Now that domed ends have been identified to be favorable design features for catalysts, it is recommended that in future studies the wall segment model should be improved. When the domed catalysts are modeled in the existing wall segment model, artificially large gaps between particles and between the catalysts and the reactor wall are created. As a result, pressure drops are unrealistically deflated and hot spots are eliminated. Effort should be devoted to developing a new reactor model for domed catalysts that more accurately reflects reality.

REFERENCES

[1] Behnam, M., A. G. Dixon, M. Nijemeisland, and E. H. Stitt. "Catalyst Deactivation in 3D CFD Resolved Particle Simulations of Propane Dehydrogenation." *Industrial & Engineering Chemistry Research* 49.21 (2010): 10641-10650. Print.

[2] Birdsall, D. J., et al. 2011. Shaped Heterogeneous Catalysts. U.S. Patent 0,172,086, filed August 24, 2009, and issued July 14, 2011.

[3] Boudreau, J. and A. Rocheleau. "Comparison of Catalyst Geometries Using Computational Flow Dynamics for Methane Steam Reforming." April 2010.

[4] Carr, M. "Computational Flow Dynamics Analysis of 5-holed Catalyst Geometries in Methane Steam Reforming." April 2012.

[5] Crabtree, G. W., M.S. Dresselhaus, and M.V. Buchanan. "The Hydrogen Economy." *Physics Today* 57.12 (2004): 39. Print.

[6] Ding, Y., and E. Alpay. "Adsorption-enhanced steam-methane reforming." *Chemical Engineering Science* 55 (2000): 3929-940. Print.

[7] Dixon, A.G., Taskin, M.E, and Stitt, E.H., "CFD Study of Fluid Flow and Heat Transfer in a Fixed Bed of Cylinders", *Numerical Heat Transfer A*, **52**, 203 (2007).

[8] Doctor and Molburg. "Hydrogen from Steam-Methane Reforming with CO2 Capture." Presented at the 20th International Pittsburgh Coal Conference Sept. 15-19, 2003.

[9] Hou, K., and Hughes, R. (2001). The kinetics of methane steam reforming over a Ni/a- Al2O catalyst. *Chemical Engineering Journal* , 311-328.

[10] Menter, F., Kuntz, M., and Langtry, R. (2003). Ten years of industrial experience with the SST turbulence model. *Proc of the 4th International Symposium on Turbulence, Heat and Mass Transfer*, 625-632.

[11] Nijemeisland, M., Dixon, A.G., and Stitt, E.H., "Catalyst design by CFD for heat transfer and reaction in steam reforming", *Chemical Engineering Science* 59 (2004): 5185-5191. Print.

[12] Taskin, M.E "CFD simulation of transport and reaction in cylindrical catalyst particles". PhD dissertation, Worcester Polytechnic Institute. August 2007.

APPENDIX A: Convergence Histories

A.1: 4H Convergence History

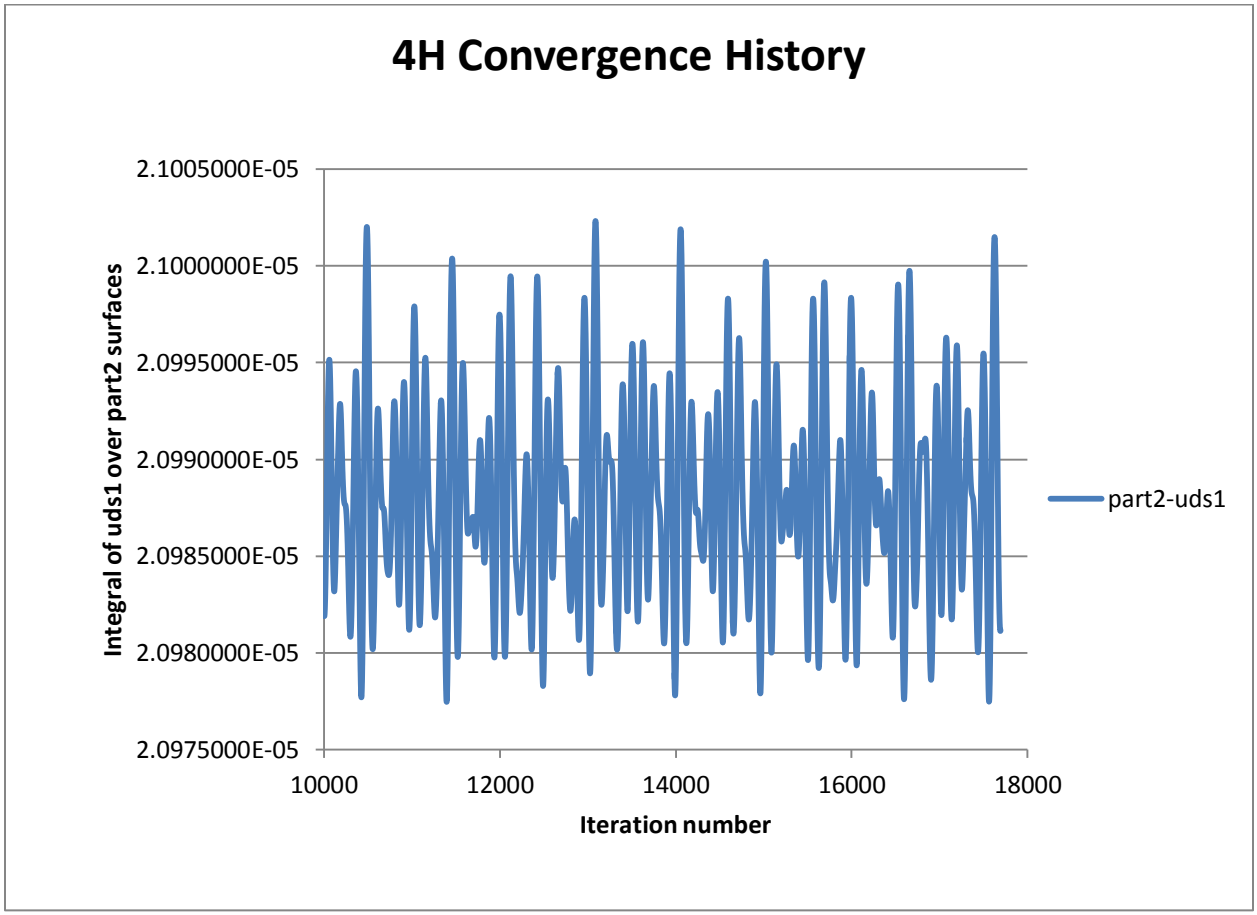

A.2: 4HG Convergence History

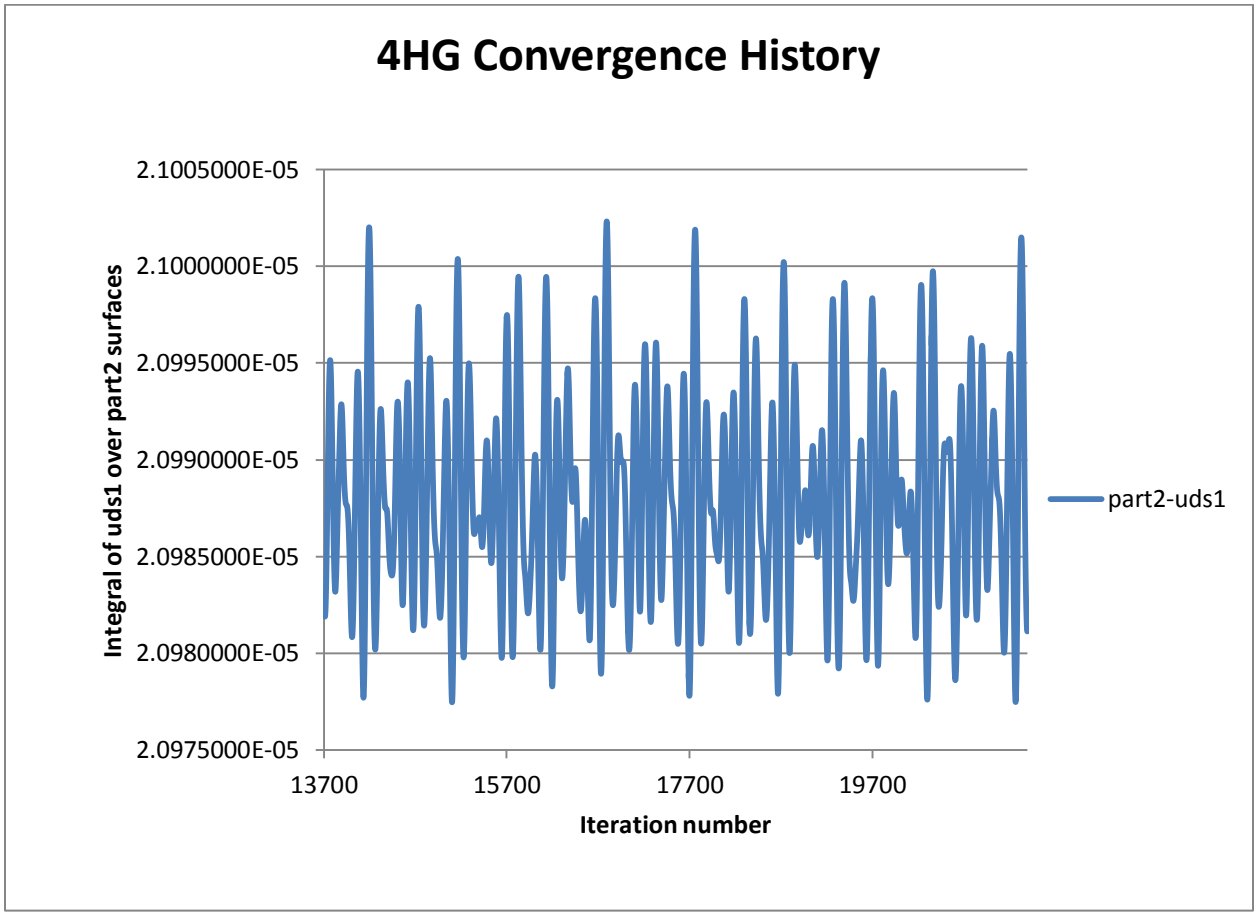

A.3: 4HGD Convergence History

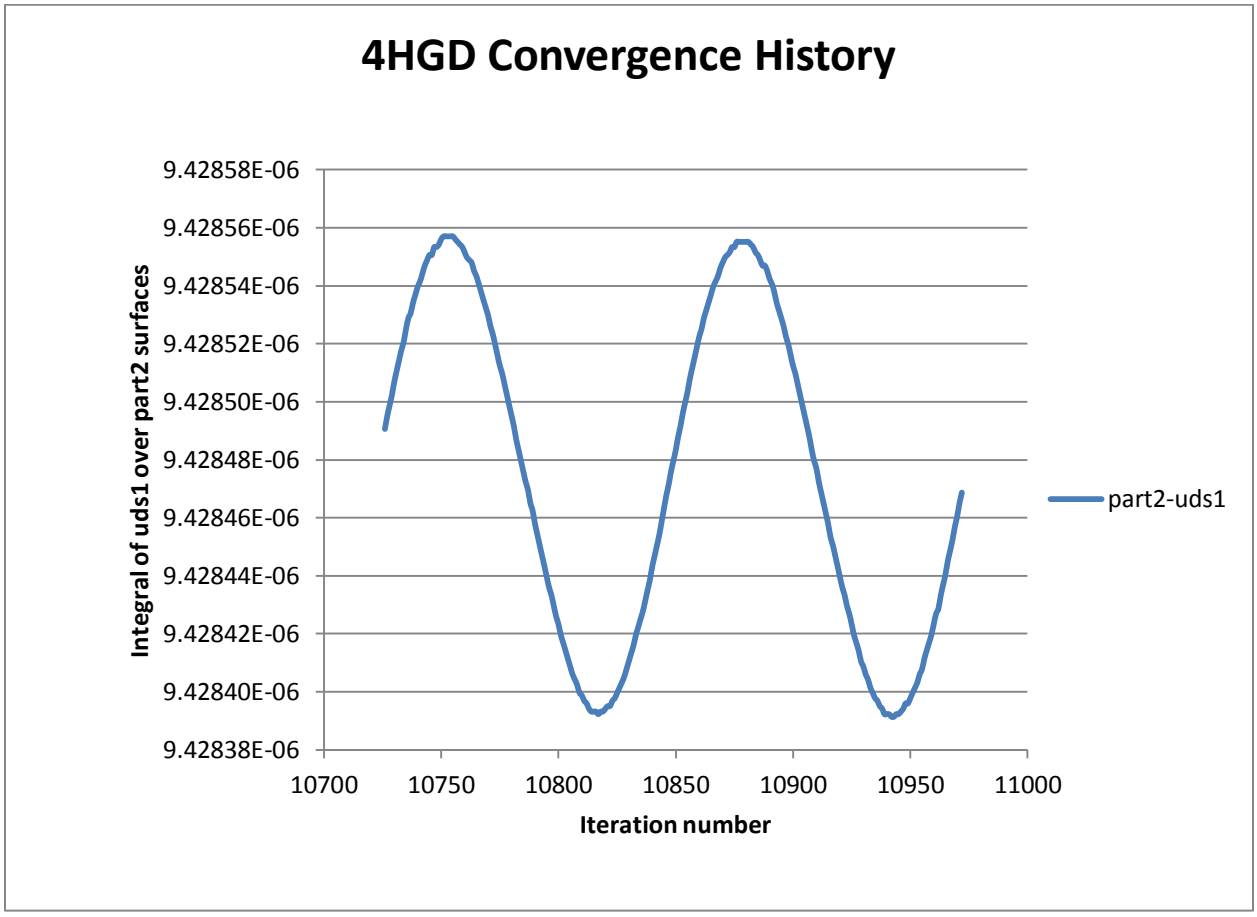

A.4: 4HD Convergence History

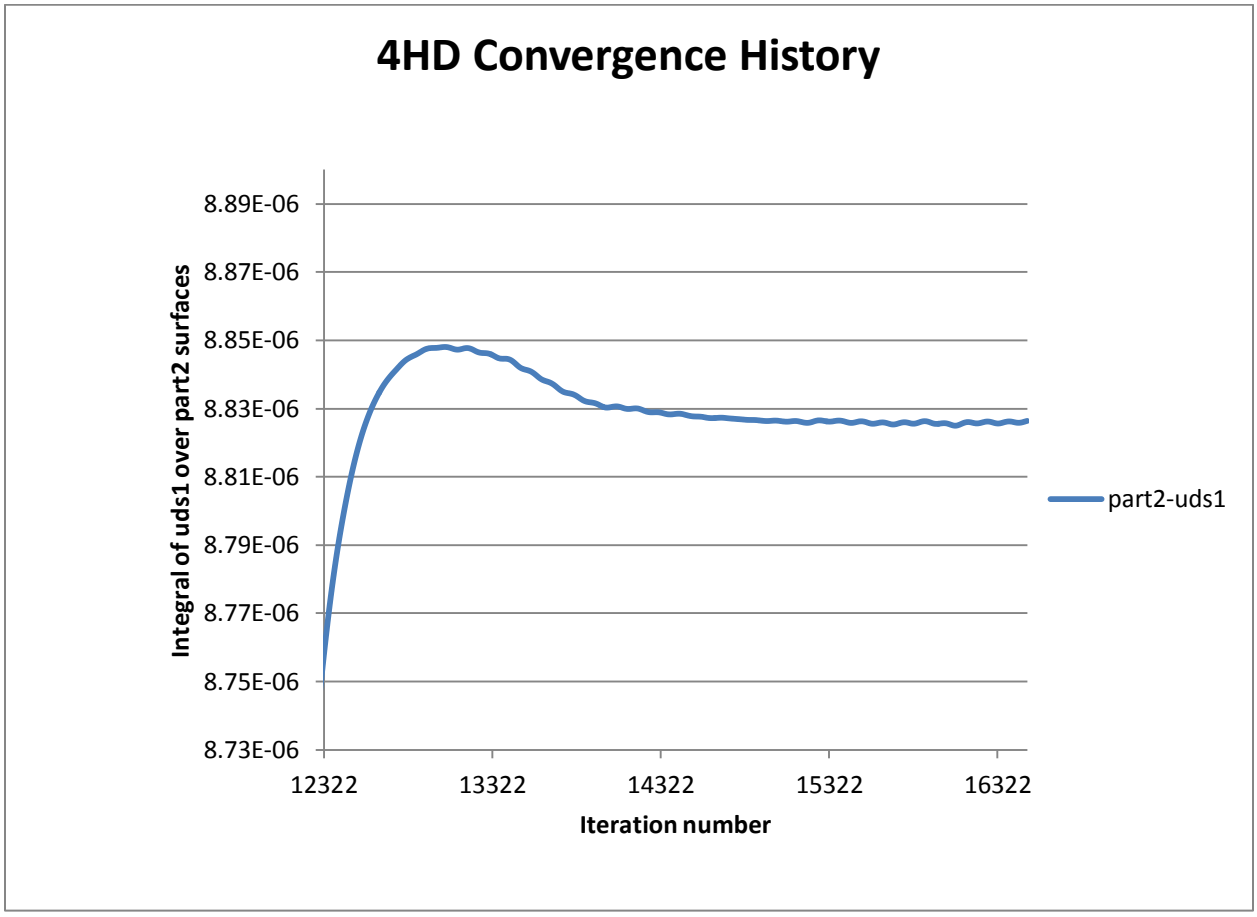

A.5: 5BHPD Convergence History

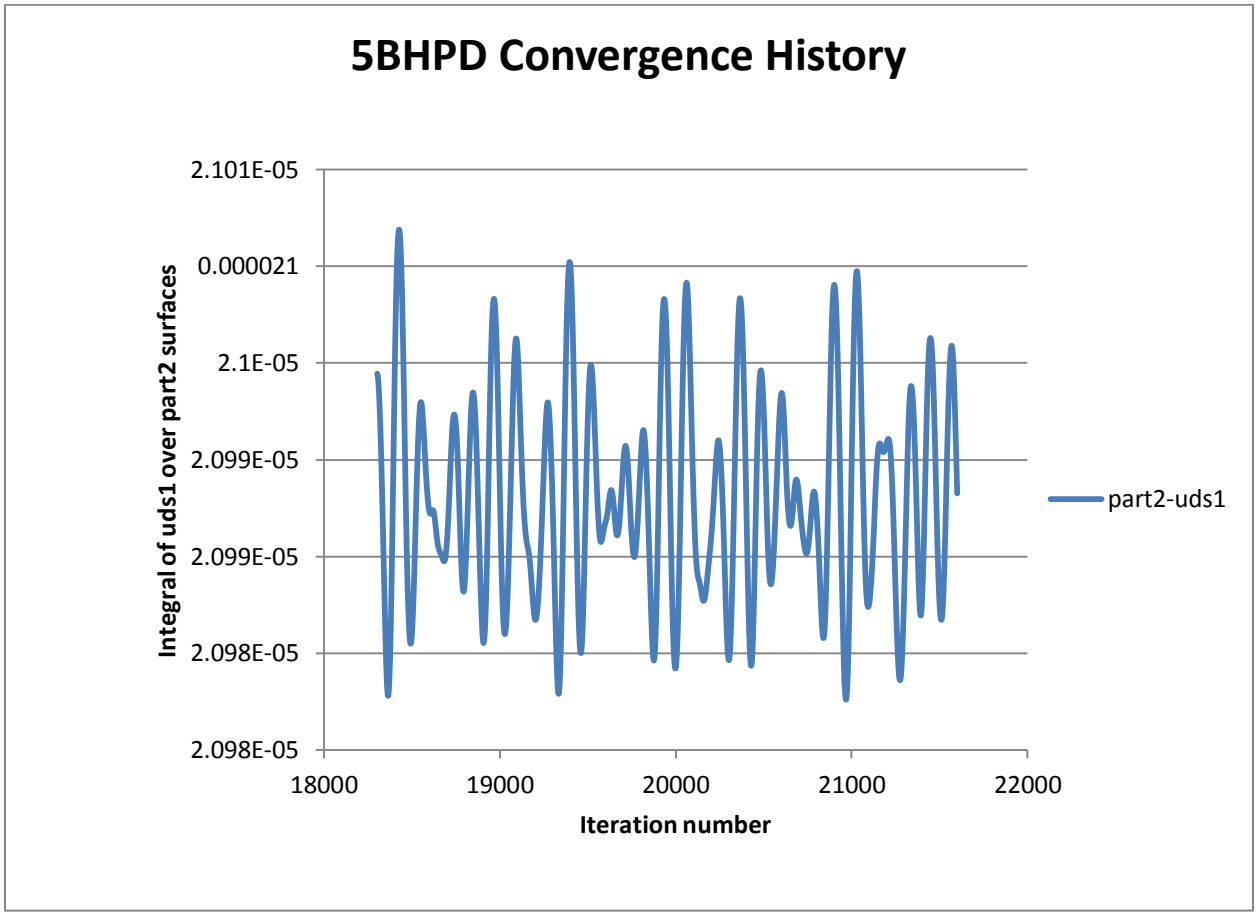

A.6: 5HP Convergence History

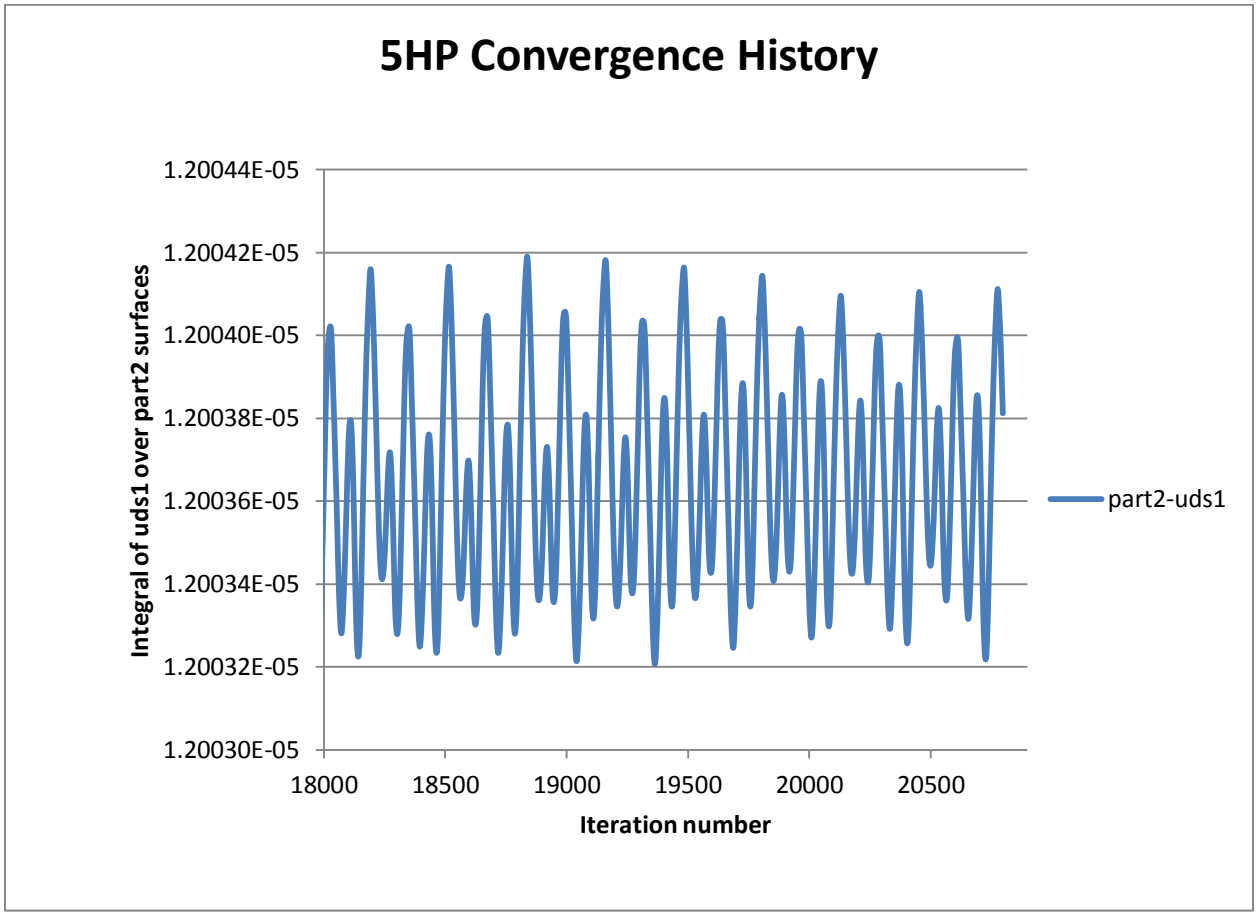

A.7: 5HPD Convergence History

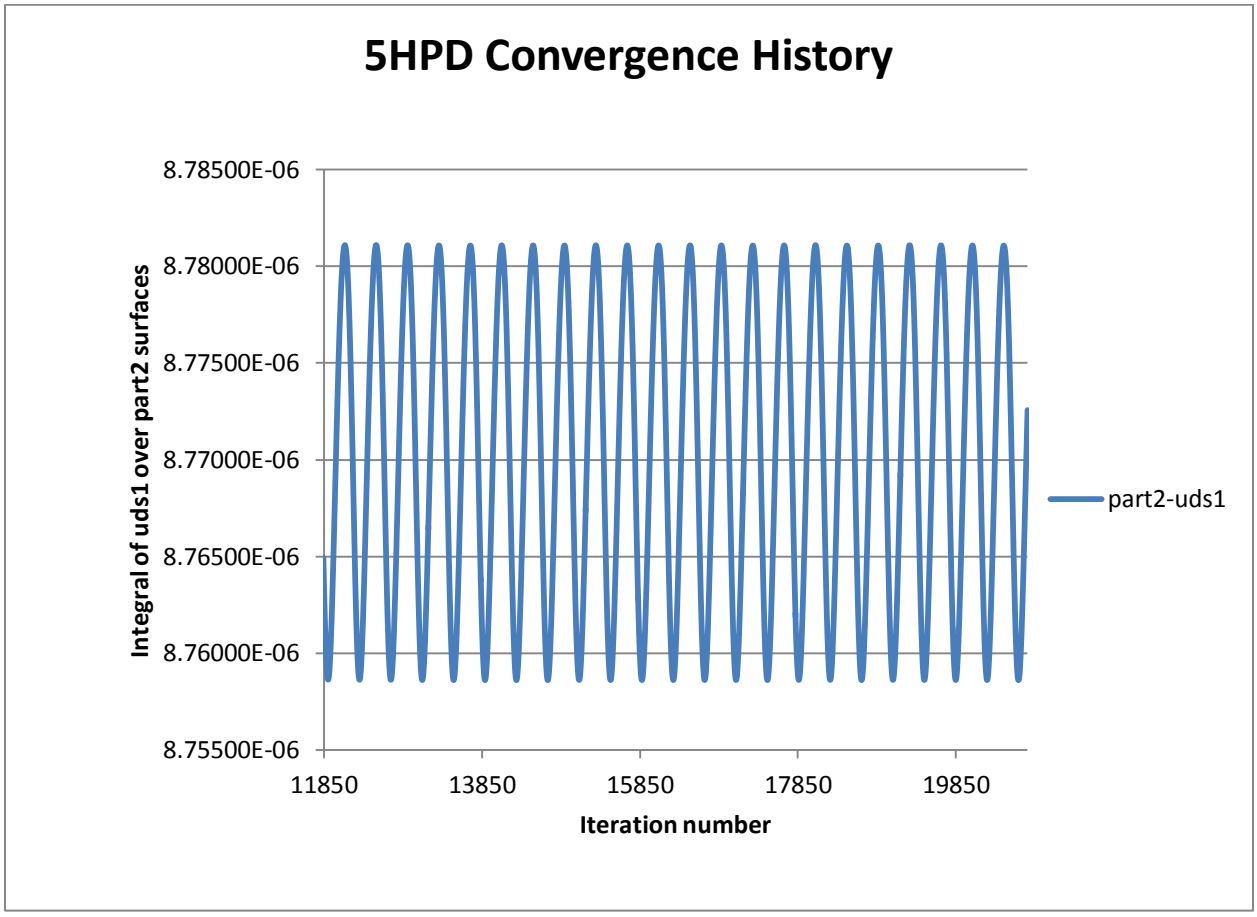

A.8: 6HG Convergence History

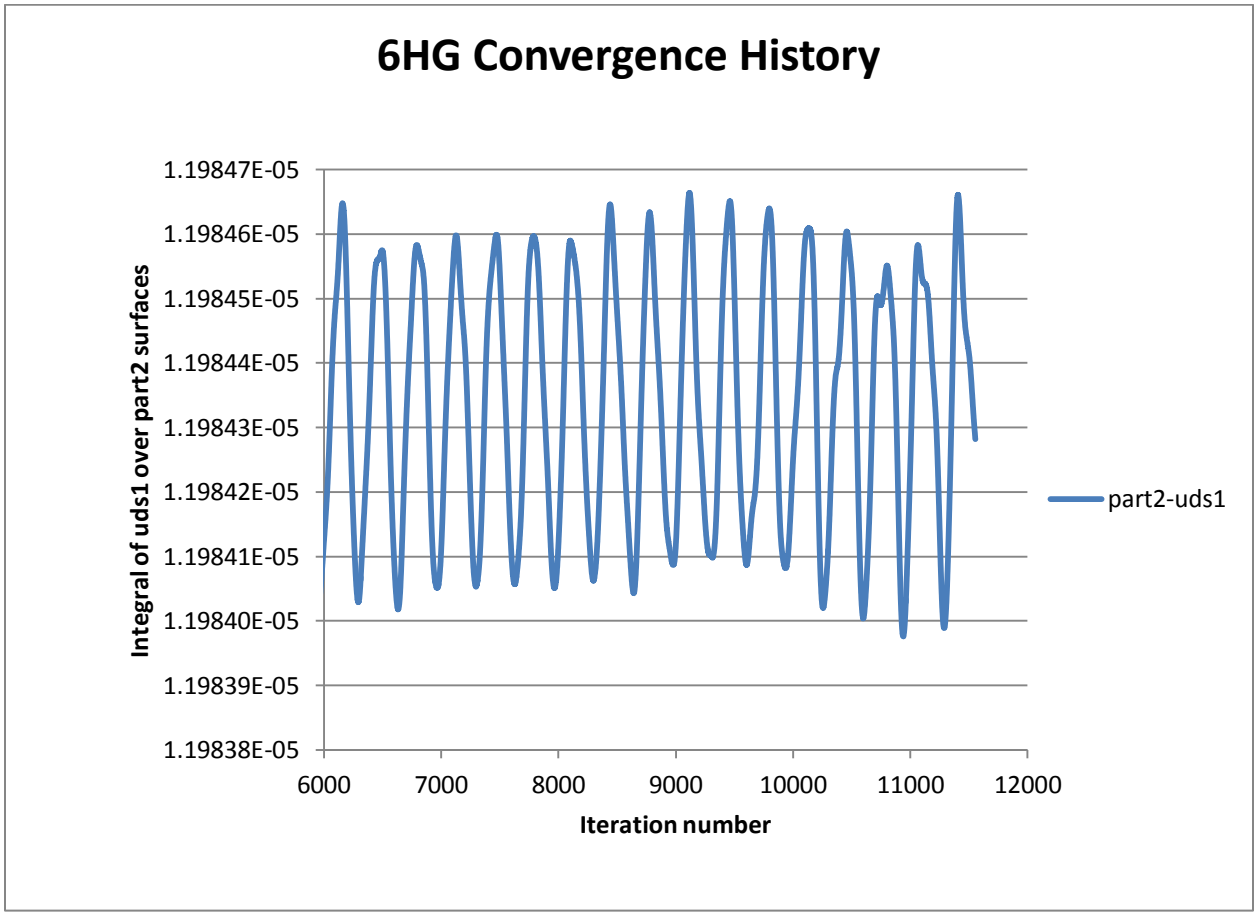

A.9: 6HGD Convergence History

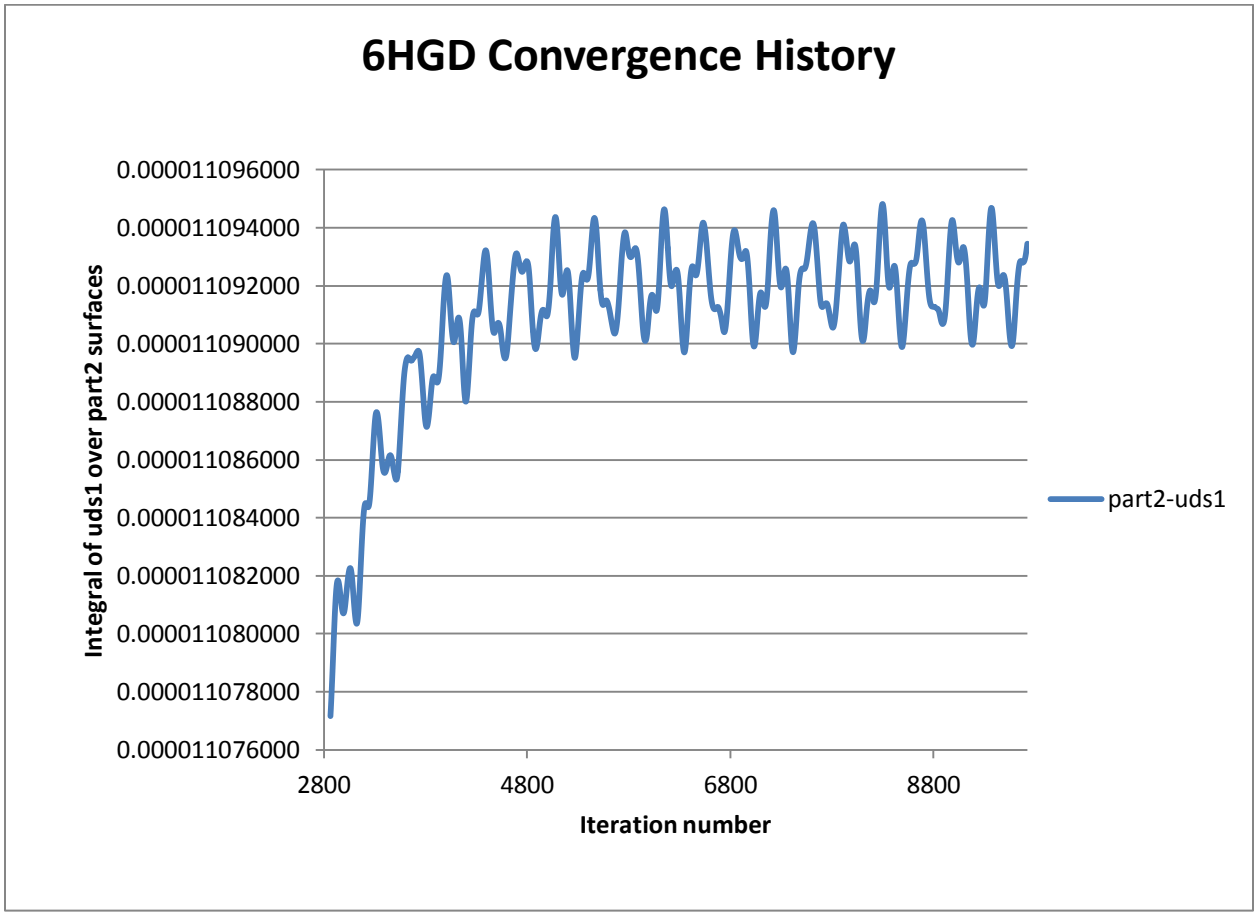

APPENDIX B: BOUNDARY LAYERS APPLIED

B.1: 4HD Boundary Layers

Volume	First layer thickness (in)	Growth	Number of layers	Total depth (in)
Wall Boundary Layer				
Cylinder	0.001	1	3	0.003
Inner Boundary Layer (into particle)				
Part2	0.001	1.2	6	0.00992992
Outer Boundary Layers (into fluid)				
Part1	0.001	1	3	0.003
Part2	0.001	1	6	0.006
Part3	0.001	1	3	0.003
Part4	0.001	1	3	0.003
Part5	0.001	1	3	0.003

B.2: 4HGD Boundary Layers

Volume	First layer thickness (in)	Growth	Number of layers	Total depth (in)
Wall Boundary Layer				
Cylinder	0.001	1	3	0.003
Inner Boundary Layer (into particle)				
Part2	0.001	1.2	6	0.00992992
Outer Boundary Layers (into fluid)				
Part1	0.001	1	3	0.003
Part2	0.001	1	6	0.006
Part3	0.001	1	3	0.003
Part4	0.001	1	3	0.003
Part5	0.001	1	3	0.003

B.3: 5HPD Boundary Layers

Volume	First layer thickness (in)	Growth	Number of layers	Total depth (in)
Wall Boundary Layer				
Cylinder	0.001	1	2	0.002
Inner Boundary Layer (into particle)				
Part2	0.002	1	2	0.004
Outer Boundary Layers (into fluid)				
Part1	0.001	1	2	0.002
Part2	0.001	1	3	0.003
Part3	0.001	1	2	0.002
Part4	0.001	1	2	0.002
Part5	0.001	1	2	0.002

B.4: 5BHPD Boundary Layers

Volume	First layer thickness (in)	Growth	Number of layers	Total depth (in)
Wall Boundary Layer				
None				
Inner Boundary Layer (into particle)				
Part2	0.002	1	2	0.004
Outer Boundary Layers (into fluid)				
Part2	0.001	1	3	0.003

B.5: 6HG Boundary Layers

Volume	First layer thickness (in)	Growth	Number of layers	Total depth (in)
Wall Boundary Layer				
Cylinder	0.001	1	2	0.002
Inner Boundary Layer (into particle)				
Part2	0.003	1	2	0.006
Outer Boundary Layers (into fluid)				
Part1	0.001	1	2	0.002
Part2	0.001	1	3	0.003
Part3	0.001	1	2	0.002
Part4	0.001	1	2	0.002
Part5	0.001	1	2	0.002

B.6: 6HGD Boundary Layers

Volume	First layer thickness (in)	Growth	Number of layers	Total depth (in)
Wall Boundary Layer				
Cylinder	0.001	1	1	0.001
Inner Boundary Layer (into particle)				
Part2	0.001	1	2	0.002
Outer Boundary Layers (into fluid)				
Part1	0.001	1	1	0.001
Part2	0.001	1	2	0.002
Part3	0.001	1	1	0.001
Part4	0.001	1	1	0.001
Part5	0.001	1	1	0.001

APPENDIX C: PARTICLE LOCATIONS

Particle	Orientation
1	R +45 +x T -1.45 +x R +40 +z
2	R -45 +x T -1.45 +x T +1 +z R +20 +z
3	C +2 +z
4	R +5 +x T -1.48 +x R -9 +z
5	C +2 +z
6	R +90 +y T -1.42 +y R +5 +z
7	C +2 +z
8	R +90 +x T -1.42 +y T +1 +z R -17.5 +z
9	R +45 +x T -1.45 +x T +1 +z R -40 +z
10	R +90 +y T -0.25 +x
11	C +2 +z
12	R +90 +x T +1 +z T -0.35 +y T +0.2 +x

R = rotate, T = translate, C = copy, h = adjust height to, r = adjust radius to. Rotations are in degrees, translations in inches. Based on a particle of 1 inch diameter and 1 inch height.

APPENDIX D: SAMPLE GAMBIT JOURNAL FILE

```
/ Journal File for GAMBIT 2.3.16, Database 2.3.14, ntx86 SP2006032921
/ Identifier "5HPDomed"
/ File opened for write dayofweek month day time year.
identifier name "yournamehere" new nosaveprevious
solver select "FLUENT 5/6"
reset
//////////////////////////////////////////////////
////////////// Creating Single Particle ////////////
//////////////////////////////////////////////////

volume create "cylinder" height 2 radius1 2 radius2 2 radius3 2 offset 0 0 1 \
  zaxis frustum
volume create "part" height 0.584 radius1 0.5 radius3 0.5 offset 0 0 0.5 zaxis frustum
volume create "TopSphere" radius 0.704961538 sphere
volume move "TopSphere" offset 0 0 0.295038462
volume split "TopSphere" faces "face.6" connected
volume delete "TopSphere" lowertopology
volume create "BottomSphere" radius 0.704961538 sphere
volume move "BottomSphere" offset 0 0 0.704961538
volume split "BottomSphere" faces "face.4" connected
volume delete "BottomSphere" lowertopology
volume create "Hole1" height 1 radius1 0.1 radius3 0.1 offset 0 0 0.5 zaxis frustum
volume move "Hole1" offset 0.25 0 0
volume cmove "Hole1" multiple 4 dangle 72 vector 0 0 1 origin 0 0 0
volume create "Flute1" height 1 radius1 0.11 radius3 0.11 offset 0 0 0.5 zaxis frustum
volume move "Flute1" offset 0.5 0 0
volume move "Flute1" dangle 36 vector 0 0 1 origin 0 0 0
volume cmove "Flute1" multiple 4 dangle 72 vector 0 0 1 origin 0 0 0
volume unite volumes "part" "volume.4" "volume.6"
volume subtract "part" volumes "Hole1"
volume subtract "part" volumes "volume.8"
volume subtract "part" volumes "volume.9"
volume subtract "part" volumes "volume.10"
volume subtract "part" volumes "volume.11"
volume subtract "part" volumes "Flute1"
volume subtract "part" volumes "volume.13"
volume subtract "part" volumes "volume.14"
volume subtract "part" volumes "volume.15"
volume subtract "part" volumes "volume.16"
volume move "part" dangle -18 vector 0 0 1 origin 0 0 0
volume move "part" offset 0 0 -0.5
```

```
/////////////////////////// Copying Particles ///////////
///////////////////////////and moving into position /////////

volume copy "part" to "part1"
volume move "part1" dangle 45 vector 1 0 0 origin 0 0 0
volume move "part1" offset -1.45 0 0
volume move "part1" dangle 40 vector 0 0 1 origin 0 0 0
volume copy "part" to "part2"
volume move "part2" dangle -45 vector 1 0 0 origin 0 0 0
volume move "part2" offset -1.45 0 0
volume move "part2" dangle 20 vector 0 0 1 origin 0 0 0
volume move "part2" offset 0 0 1
volume copy "part1" to "part3"
volume move "part3" offset 0 0 2
volume copy "part" to "part4"
volume move "part4" dangle 5 vector 1 0 0 origin 0 0 0
volume move "part4" offset -1.48 0 0
volume move "part4" dangle -9 vector 0 0 1 origin 0 0 0
volume copy "part4" to "part5"
volume move "part5" offset 0 0 2
volume copy "part" to "part6"
volume move "part6" dangle 90 vector 0 1 0 origin 0 0 0
volume move "part6" offset 0 -1.42 0
volume move "part6" dangle 5 vector 0 0 1 origin 0 0 0
volume copy "part6" to "part7"
volume move "part7" offset 0 0 2
volume copy "part" to "part8"
volume move "part8" dangle 90 vector 1 0 0 origin 0 0 0
volume move "part8" offset 0 0 1
volume move "part8" offset 0 -1.42 0
volume move "part8" dangle -17.5 vector 0 0 1 origin 0 0 0
volume copy "part1" to "part9"
volume move "part9" offset 0 0 1
volume move "part9" dangle -40 vector 0 0 1 origin 0 0 0
volume move "part9" dangle -40 vector 0 0 1 origin 0 0 0
volume copy "part" to "part10"
volume move "part10" dangle -45 vector 0 1 0 origin 0 0 0
volume move "part10" offset -0.25 0 0
volume copy "part10" to "part11"
volume move "part11" offset 0 0 2
```

```
volume copy "part" to "part12"
volume move "part12" dangle 90 vector 1 0 0 origin 0 0 0
volume move "part12" offset 0 0 1
volume move "part12" offset 0.2 0 0
volume move "part12" offset 0 -0.35 0
volume delete "part" lowertopology


////////////////////////////////////////////////////////////////////////
////////////// Creating volume "tool" to split tube into 120 degree segment//////
////////////////////////////////////////////////////////////////////////

volume create "b1" width 3 depth 3 height 4 offset 1.5 1.5 2 brick
volume move "b1" offset 0 0 -1
volume copy "b1" to "b2"
volume move "b2" dangle 60 vector 0 0 1 origin 0 0 0
volume copy "b1" to "b3"
volume move "b3" dangle -90 vector 0 0 1 origin 0 0 0
volume copy "b1" to "b4"
volume move "b4" offset -3 0 -3
volume copy "b4" to "b5"
volume move "b5" offset 0 -3 0
volume copy "b5" "b4" to "b6" "tool"
volume move "b6" "tool" offset 0 0 6
volume unite volumes "tool" "b6" "b4" "b5" "b2" "b1" "b3"
/ Modification to W geometry
volume move "tool" dangle -1 vector 0 0 1 origin 0 0 0
volume move "part1" "part2" "part3" "part4" "part5" "part6" "part7" "part8" \
  "part9" "part10" "part11" "part12" offset 0 0 0.04
/ Trim cylinder and the eleven particles that stick out of the segment
volume subtract "cylinder" volumes "tool" keeptool
volume subtract "part7" volumes "tool" keeptool
volume subtract "part3" volumes "tool" keeptool
volume subtract "part11" volumes "tool" keeptool
volume subtract "part5" volumes "tool" keeptool
volume subtract "part4" volumes "tool" keeptool
volume subtract "part1" volumes "tool" keeptool
volume subtract "part10" volumes "tool" keeptool
volume subtract "part6" volumes "tool" keeptool
volume subtract "part12" volumes "tool" keeptool
volume subtract "part8" volumes "tool" keeptool
volume subtract "part9" volumes "tool"
/Split cylinder with particles to avoid connecting faces
volume split "cylinder" volumes "part1" "part2" "part3" "part4" "part5" \
```

"part6" "part7" "part8" "part9" "part10" "part11" "part12" connected

////////////////////////////////////
/Label all faces for future reference/
////////////////////////////////////

/Modify Face labels in order to refer to them later/

//////////////////////////////////////
/ FACE LINKING /
//////////////////////////////////////

/Link all faces on the top and bottom of the geometry to create periodic zone

//////////////////////////////////////
/ Boundary and Continuum Types /
//////////////////////////////////////

/Define Fluid/solid volumes and boundary types in this section

//////////////////////////////////////
/ BLs /
//////////////////////////////////////

/Define Boundary Layer information for any boundary layers which are needed

////////////////////////////////////
/ MESH
////////////////////////////////////

/Input meshing details for geometry here

/Write out the mesh
export fluent5 "5HPDomed.msh"